Progress in Aerospace Sciences 105 (2019) 98–125

Contents lists available at ScienceDirect

Progress in Aerospace Sciences

journal homepage: www.elsevier.com/locate/paerosci

Space traffic management: towards safe and unsegregated space transport operations

Samuel Hilton[a], Roberto Sabatini[a,*], Alessandro Gardi[a], Hideaki Ogawa[a], Paolo Teofilatto[b]

[a] RMIT University – School of Engineering, Aerospace Engineering and Aviation, Bundoora, Victoria, 3083, Australia
[b] School of Aerospace Engineering – Sapienza University of Rome, Via Salaria 851, 00184, Rome, Italy

ARTICLE INFO

Keywords:
Space traffic management
Space transport
Air traffic management
Avionics
Aerospace electronic systems
Aerospace information systems
Cyber-physical systems
Unmanned reusable space vehicle
Air traffic flow management
Autonomous systems
Safety analysis
Space debris
Collision avoidance

ABSTRACT

Progress in spaceflight research has led to the introduction of various manned and unmanned reusable space vehicle concepts, opening up uncharted opportunities for the newborn space transport industry. For future space transport operations to be technically and commercially viable, it is critical that an acceptable level of safety is provided, requiring the development of novel mission planning and decision support tools that utilize advanced Communication, Navigation and Surveillance (CNS) technologies, and allowing a seamless integration of space operations in the current Air Traffic Management (ATM) network. A review of emerging platform operational concepts is conducted, highlighting both the challenges and the opportunities brought in by the integration with conventional atmospheric air transport. Common launch and re-entry planning methodologies are then discussed, where the physical and computational limitations of these approaches are identified and applicability to future commercial space transport operations is assessed. Attention is then turned to the on-orbit phase, where the unique hazards of the space environment are examined, followed by an overview to the necessary elements required for space object de-confliction and collision avoidance modelling. The regulatory framework evolutions required for spacecraft operations are then discussed, with a focus on space debris mitigation strategies and operational risk assessment. Within the atmospheric domain, possible extensions and alternatives to the conventional airspace segregation approaches are identified including promising Air Traffic Flow Management (ATFM) techniques to facilitate the integration of new-entrant platforms. Lastly, recent modelling approaches to meet on-orbit risk criteria are discussed and evolutionary requirements to improve current operational procedures are identified. These insights will inform future research on CNS/ATM and Avionics (CNS + A) systems and associated cyber-physical architectures for Space Traffic Management (STM).

1. Introduction

Capitalising on lessons learned from the Space Shuttle era, various manned and unmanned reusable space vehicle concepts have been proposed in recent years and some of these concepts are now being developed and successfully tested. Moving away from the traditional approach of expendable launch vehicles, the capability of reusable launch systems are currently being demonstrated by companies such as SpaceX and Virgin Galactic. Reusable platforms provide clear economic advantages and are now widely recognised as an integral component of a sustainable space transportation industry. These so called "new-entrants" push the envelope in regards to how the various flight phases are accomplished, introducing concepts such as Vertical Take-Off and Landing (VTOL), Horizontal Take-Off and Landing (HTOL) and hybrid approaches [1–5].

As the new-entrant technologies are being increasingly realised, the aviation and space industry (to a lesser extent) are undergoing large scale modernisation processes towards increasing capacity, safety and efficiency. It is well understood that this will require the establishment of a Space Traffic Management (STM) system as well as a significant evolution from ground-based legacy systems realizing an advanced global network of Communication, Navigation and Surveillance (CNS) technologies [6–8]. As such, the integration of avionics CNS technologies into new-entrant platforms will be a critical aspect, associated to simultaneous development of new air/ground mission planning and decision support tools that harmonize future Air Traffic Management (ATM) and spacecraft operational procedures. Within the orbital domain, Space Situational Awareness (SSA) is being provided by a network of ground based surveillance systems known as the Space Surveillance Network (SSN) operated by the US Department of Defense.

* Corresponding author.
E-mail address: roberto.sabatini@rmit.edu.au (R. Sabatini).

https://doi.org/10.1016/j.paerosci.2018.10.006
Received 25 October 2018; Accepted 30 October 2018
Available online 06 February 2019
0376-0421/

Nonetheless, a shift is now being pursued towards establishing a more "global" surveillance approach through both spaceborne measurements and Resident Space Object (RSO) data sharing from other commercial and governmental entities [9–11]. Emerging capabilities such as this pave the way for implementing the evolutionary changes required for a globally harmonised ATM/STM system.

Unlike conventional aircraft, new-entrants will operate in severe environments at extremely high velocities and as such the design and development of future ATM/STM operational procedures must consider the limitations each phase/environment imposes. The launch and re-entry environment is characterized by significant platform constraints regarding aerodynamic loading and thermal stresses [12–14]. Since the shuttle orbiter, re-entry planning schemes based on the use of the Quasi Equilibrium Glide Condition (QEGC) [15–19] and energy methods [20,21] have been developed and tested.

During the on-orbit phase, spacecraft are subject to an environment that distinctly differs from that on the Earth. Space weather phenomena is not only hazardous to human life [22–24] but has the potential to significantly degrade the performance of advanced CNS equipment [14,25–28]. The highly non-linear dynamics of perturbed orbital motion is also an important issue that must be considered, especially because it affects the validity of the long-term predictions required to assure separation from other spacecraft (operational and non-operational) and debris. Thus adequate measures must be implemented to accurately describe position uncertainty and its propagation over time. Common approaches to this problem are identified and discussed, including novel methods that aim to unify the approach to uncertainty representation in the interest of STM/ATM harmonisation and platform interoperability [29,30].

In lieu of a harmonised ATM/STM system, various international and national organisations have developed guidelines and standards to mitigate the risks associated with spaceflight operations [31–35]. Within the atmospheric domain, safety criteria have been met to date through ad-hoc approaches that segregate space transport vehicles from atmospheric aircraft during the launch and re-entry phases. Although relatively effective in current airspace, the applicability of such conservative approaches to future mixed flow operations is questionable. As a result, novel methods have been proposed to achieve an optimized hazard volume based on spacecraft design characteristics and predetermined trajectories [36,37]. Alongside promising Air Traffic Flow Management (ATFM) concepts [38] these methods have the potential to be strongly beneficial to future mixed-flow operations. However, the increasingly problematic situation of space debris has raised concerns about the sustainability of the orbital environment [39,40]. As a consequence, mitigation guidelines outlining disposal strategies have been developed to slow the growth of debris within the Low Earth Orbit (LEO) and Geosynchronous (GEO) regions. These strategies are now evolving to meet both current and predicted operational compliance requirements [41–43]. However, as of now, it is clear that active measures must be also taken by spacecraft operators to identify potential on-orbit collisions and perform timely de-confliction manoeuvres.

Based upon on-orbit uncertainty modelling, various analytical tools have been developed to allow spacecraft operators to assess risk and meet the required operational criteria [44–50]. However, recent events, such as the 2009 collision between the Iridium 33 and Cosmos spacecraft, have demonstrated that unreliable observational data introduce significant additional uncertainties that impact on the overall validity of current safety assessment methods. This paper identifies the common modelling approaches taken to conduct on-orbit collision avoidance analysis addressing both the challenges and the necessary evolutions to increase the transparency and traceability of observational data required for future STM operations.

2. Communication, navigation and surveillance within the ATM/STM domain

Aviation is undergoing a large-scale modernisation process, in which the state-of-the-art in aeronautical technology and higher levels of automation and information sharing are exploited to increase the safety, capacity, efficiency and environmental sustainability of air traffic [38,51,52]. Several major programs were launched to guide and support this modernisation, including the US Next Generation Air Transportation System (NextGen) and the Single European Sky ATM Research (SESAR) and other programs such as CARATS (Collaborative Actions for Renovation of Air Traffic Systems) in Japan and OneSky in Australia. These programs focus on novel operational capabilities and enabling technologies to meet future air transportation challenges including civil/military air traffic harmonisation and, more recently, UAS access to all classes of airspace. The NASA UAS Traffic Management (UTM) research initiative is currently leading the way in this direction, working with various academic, industrial and government institutions on prototype CNS/ATM and Avionics (CNS + A) technologies addressing airspace integration requirements for safe and efficient UAS operations [53–58]. The new services conceived in the UTM concept-of-operation will provide to UAS pilots information for maintaining separation from other aircraft by reserving airspace portions, with consideration of special use airspace and adverse weather conditions [56]. Consequently, the current operational concept mostly relies on opportune provisions for airspace design and management, geo-fencing, congestion management, authenticated operations and weather prediction services to provide an effective and seamless integration of UAS in the current ATM network. These provisions aim at reducing the potential risks to an acceptable level but it is now clear that a certifiable Sense-and-Avoid (SAA) capability is integral to a proper management of the risks throughout the entire operational spectrum of UAS platforms [59–61].

All these research initiatives are driving the advancement of CNS + A technologies towards allowing increased operational efficiency and safety in the management of air traffic and airspace resources, thereby providing technically viable and effective long-term solutions to cope with the global increase in air transport demand [6–8]. A key challenge for the future will be the global harmonisation of the ATM/UTM and STM frameworks, including the development of a cohesive certification framework for future CNS + A systems simultaneously addressing safety, security and interoperability requirements [62].

2.1. Towards performance based operations

Continuing rapid advances in aerospace sensor and computing technologies are stimulating the development of integrated and multi-sensor systems capable of providing to the pilot, in a synthetic form, all information required for a safe and accurate navigation. Furthermore, automatic control and networking technologies have been extensively applied to Unmanned Aircraft Systems (UAS), allowing the development of multisensor systems for fully-automated aircraft guidance. The recent introduction of Performance-Based Navigation (PBN) is the first step of an evolutionary process from equipment-based to Performance-Based Operations (PBO). PBN specifies that aircraft navigation systems performance requirements shall be defined in terms of accuracy, integrity, availability and continuity for the proposed operations in the context of a particular airspace, when supported by an appropriate ATM infrastructure. The full PBO paradigm shift requires the introduction of suitable metrics for Performance-Based Communication (PBC) and Performance-Based Surveillance (PBS). The proper development of such metrics and a detailed definition of PBN-PBC-PBS interrelationships for manned and unmanned aircraft operations represent one of the most exciting research challenges currently faced by the avionics research community, with major impacts on air transport safety, airspace capacity and operational efficiency.

Despite being a core technology enabler for high-density and uncertainty-resilient operations, advanced communication systems have not experienced the same rapid uptake observed in aeronautical navigation and surveillance technologies. For instance, current communications between conventional aircraft and ground entities (ATM, airlines and airport authorities) are still heavily reliant on analogue voice channels. The progressive introduction of digital data links and other networking technologies is now allowing a much enhanced timeliness and reliability of traffic flow information, increasing productivity and streamlining system capacity. At the core of this transformation, System-Wide Information Management (SWIM) will constitute the backbone of the data communication concept, providing the network to share strategic and tactical information, enabling new modes of decision making for safety-critical air/space traffic management concepts such as Trajectory Based Operations (TBO).

Surveillance systems are designed to support traffic separation assurance and collision avoidance functions. Cooperative surveillance systems use a combination of Time and Space Position Information (TSPI) and communication links to share traffic information between aircraft and ground-based ATM systems. Non-cooperative systems can include radar, electro-optical and other kind of active/passive sensors using various working principles and operating in various portions of the radiofrequency, infrared and/or visible spectrum [59,63,64]. The state-of-the-art in avionics surveillance is the Automatic Dependent Surveillance Broadcast (ADS-B) system. This is a cooperative system using TSPI from Global Navigation Satellite Systems (GNSS) and existing aeronautical data links. ADS-B provides significantly higher amounts of information compared to conventional Primary Surveillance Radar (PSR) and Mode-C Transponders, hence supporting a greatly enhanced situational awareness for air traffic controllers and pilots.

The integration of the above CNS + A technology into spacecraft platforms will be a critical aspect in performing more “aircraft like” operations, allowing the transition from segregated to mix flow operations. Understandably, spaceflight will not only require CNS equipment to be highly reliable and light weight but also highly robust due to the extreme operating environments experienced through various flight phases.

2.2. Global CNS infrastructure

A future harmonised ATM/STM system will require unprecedented levels of situational awareness, which can only be achieved with new data analytics methods and a globally connected infrastructure. In the aviation context, the distinct advantages of employing global satellite systems have been widely demonstrated by GNSS (with its augmentation systems), allowing airspace capacity, route efficiency and safety to be significantly increased [65–67]. Similarly, for the full potential of advanced surveillance and communication technology to be realised, the development of new global satellite-based services will be required.

2.3. Space Situational Awareness

Space Situational Awareness (SSA) refers to the knowledge of the near space environment, which in the context of STM is largely concerned with the knowledge of RSO information. Effective SSA requires constant surveillance and tracking of the space environment, a task traditionally performed by a network of ground based observation facilities known as the Space Surveillance Network (SSN), owned and operated by the US Department of Defence (DoD). However, over the past decade a shift towards a global surveillance approach of SSA data sources has been possible as commercial entities and other countries exhibiting SSA capabilities that match or exceed the US DoD [9].

Albeit, ground based radar, laser and telescope systems will continue to provide a pivotal role in providing situational awareness of the space environment, however the feasibility of conducting space-borne measurements has been identified [10,11]. This is credit of on board sensors ability to offer greater performances in terms of accuracy, larger field of view and weather independency allowing space-borne measurements to provide a wider set of useful observations [68]. Further, space based observation systems are not subject to the scattering, diffraction, turbulences and aberrations that exist within the atmosphere [69]. The use of radar sensors to provide space-borne measurements has been explored in the past, however due to challenges associated with size & power consumption, there has been a shift in research towards optical based systems. Technological advancements in optical sensor principles (*e.g.* Coupled Charged Device (CCD) [11], complementary metal–oxide–semiconductor (CMOS), photon counting sensors [68,70]) have significantly increased optical detection performance, demonstrating the ability to track a 3 cm diameter object at a 3000 km range [68,71].

Nevertheless, orbital estimation via optical tracking is a difficult task due to the relatively limited field of view the sensors offer and the subsequent extremely short observation arc. To address this problem, the use of multi-space craft approach has been proposed [68]. This concept uses a formation of coordinated spacecraft to work in synergy and compile tracking and estimation data to obtain more accurate and complete situational awareness.

3. Categorisation of new-entrant platforms

A variety of new space platforms have been recently proposed that bend the traditional image and classification of space vehicles [1–5]. Space platforms can be categorised into expendable launch vehicles (ELVs) and reusable launch vehicles (RLVs). Historically, a vast majority of space missions have relied on ELVs but RLVs are recently drawing great interest due to the remarkable potential economic savings [72,73]. For instance, important savings were eventually achieved by the Falcon 9 (SpaceX) that now stands as a successful case study and is setting the new standard for space access costs [74,75]. Development of other cost-effective reusable systems is currently underway including endeavours by Virgin Galactic (SpaceShipTwo + WhiteKnightTwo) and Reaction Engines (Skylon) [76,77]. In addition to the RLV/ELV classification, space systems are also categorised based on their take-off and landing operational layout, as detailed in the following sub-sections.

3.1. Vertical take-off and landing

Vertical take-off is regarded as the traditional approach for space launch. In multistage configurations (*e.g.*, Space X Falcon 9) the upper stage can achieve orbital insertion while the first stage is recovered via vertical landing [74,75], as schematically depicted in Fig. 1 for a typical two-stage VTOL platform. Unmanned RLVs such as the SpaceX Falcon 9

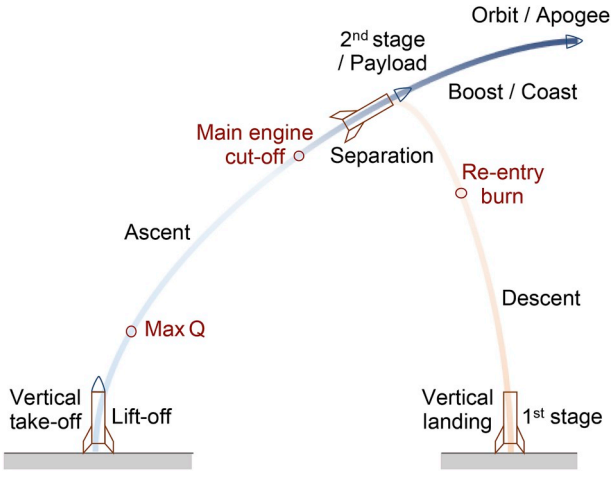

Fig. 1. VTOL platform schematic (two stages).

and Blue Origin's New Shepard achieved reusability by incorporating platform stabilizing fins and retrograde propulsion techniques to support vertical landing via thrust control [2,12,74]. A suborbital VTOL vehicle concept recently proposed is the hyper-velocity intercontinental transport system recently announced by SpaceX [78–80].

VTOL spacecraft concepts for suborbital transport mostly entail a ballistic phase and are considered a staple case for future space traffic management [80]. From the atmospheric ATM perspective, the main advantage of the VTOL vehicles is that the atmospheric transits during both ascent and descent occur in the quickest possible manner, so that their interference with atmospheric traffic is relatively limited in time, as further discussed later. However, the launch, ballistic and re-entry phases of VTOL platforms offer very limited manoeuvring margins as these platforms do not rely on aerodynamics for lift, stability or flight control and their thin shelled structure would potentially disintegrate in case of significant lateral accelerations, therefore their manoeuvrability is substantially negligible [81], so they cannot be considered an active player in any de-confliction or collision avoidance processes.

In orbital flight, the spacecraft and/or payload transported by launch vehicles are typically placed in LEO as the final orbit for LEO missions. For non-LEO mission, LEO serves as a parking orbit from which the spacecraft/payload is further transferred to a larger elliptic orbit including MEO, HEO and GEO, or parabolic/hyperbolic transfer orbit for lunar, interplanetary and deep-space missions. This decade has seen growing interest in low-mass payload launchers to transport mini/micro satellites for scientific and academic missions (*e.g.*, CubeSats) and constellation satellites primarily for commercial and strategic applications. Low-cost launchers for small payload are actively developed worldwide including, Rocket Lab's Electron, Firefly α, and Virgin Galactic's LauncherOne [82,83].

3.2. Horizontal take-off and landing

In contrast to VTOL, horizontal take-off and landing (HTOL) platforms are significantly more accommodating in their integration to conventional air traffic. Suborbital HTOL platforms are expected to enable next-generation, point-to-point transport systems for intercontinental travel, as explored extensively in the past programs for suborbital airplanes such as NASP and HOTOL [78–80]. Fig. 2 shows a schematic of a generic HTOL platform comprising two stages.

Increasing commercial attention in affordable space tourism and small payload launch capabilities has led to renewed interest in HTOL platforms. Examples of contemporary HTOL concepts include XCOR and Skylon platforms under development by XOR Aerospace and Reaction Engines, respectively, as well as the SpaceLiner concept by DLR [5,12,84]. Unlike the ballistic nature of suborbital VTOL platforms, the SpaceLiner and Skylon HTOL concepts exploit aerodynamics to generate lift and control forces in their atmospheric transits both during ascent and during re-entry. The Earth's atmosphere is also exploited for air-breathing propulsion, which relieves the platform from the need of carrying vast amounts of oxidiser.

HTOL platforms, like all other vehicles, typically rely on multi-stage launch systems, especially for orbital flight. Air launch systems are a subclass of multi-stage HTOL launch systems. Examples include North American X-15, Virgin Galactic's SpaceShipTwo and Orbital ATK's Pegasus, where a subsonic/transonic aircraft with air-breathing propulsion is used as a carrier (first stage), and the second/upper stage(s) are separated and launched in air to space, powered by solid/hybrid propellant rocket motors [76,83,85] [76,86,87]. Reaction Engines' Skylon concept is an exception of orbital HTOL, targeting single-stage-to-orbit (SSTO) by using the SABRE combined-cycle propulsion technology consisting of a turbo-ramjet and rocket engines [77,88].

3.3. Hybrid

By definition, hybrid platforms are a combination of the VTOL and HTOLapproaches, examples being the Space Shuttle Orbiter and Sierra Nevada Corporation's Dream Chaser platforms [74–76,86,87]. Requiring a vertical take-off with solid rocket boosters, these platforms are limited in manoeuvrability during their ascent, however during re-entry and subsequent gliding flight below FL600 their lifting body and control surfaces allows a significant level of manoeuvrability (Fig. 3). Hybrid platforms typically utilize winged configurations for the reusable stage to exploit aerodynamic forces for flight stability and control.

4. Operational phases

Beyond the highly vertical flight envelope – as opposed to atmospheric traffic – technical difficulties of integrating space vehicle activities with the conventional ATM infrastructure primarily originate from the significantly higher energy requirements, which exacerbate airworthiness certification challenges, as well as with the inherent manoeuvrability limitations discussed so far. Space platforms are designed to operate at extremely high-velocity in severe environments and frequently feature reduced manoeuvrability due to a lack of aerodynamic controls and/or scarce propellant. Other important technical challenges include high position uncertainties due to complex aerothermal interactions and to the high variability of the atmospheric environment, orbital perturbations associated with space weather and environment and the increasing probability of collision with space debris and the ever-growing government and commercial space activities [23,24].

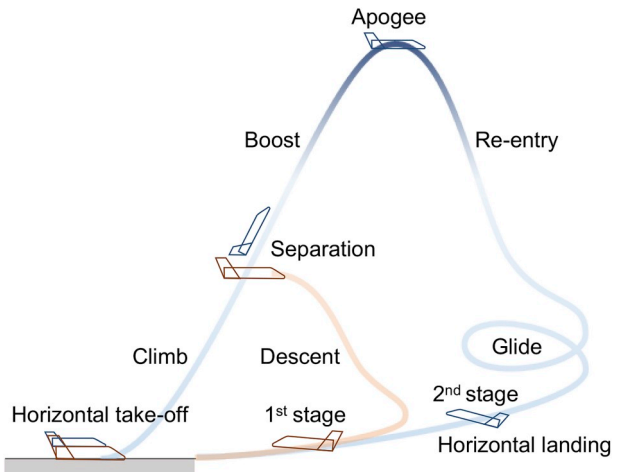

Fig. 2. HTOL platform schematic (two stages).

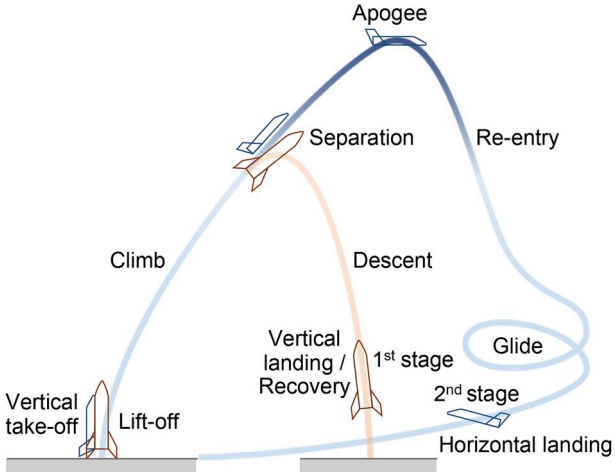

Fig. 3. Hybrid platform schematic (two stages).

These and other specificities must be thoroughly considered as part of the technological requirements for ATM/STM integration and shall be carefully considered in all planning and operational processes. As a consequence, a solid understanding of the physical characteristics of each flight phase is a prerequisite for achieving ATM/STM harmonisation.

4.1. Launch

In the course of launch and ascent, space vehicles are subjected to severe dynamic, aerodynamic, and thermodynamic environments, as described below, which crucially constrain the design and operation of the launch vehicles and payload [14]. Manned launch systems require careful assessment of the risk of ascent aborts associated with failure environments such as debris strikes and blast overpressure from explosion in the event of a launch vehicle failure during the ascent phase [89].

4.1.1. Propulsion systems

The propulsion systems of launch vehicles can be categorised into two classes, namely rocket and air-breathing engines, depending on the source of the oxidiser, *i.e.*, if it is carried as a propellant (rocket) or supplied by oxygen in atmosphere (air-breathing).

Rocket engines produce thrust by burning liquid or solid propellants, or their combination (hybrid propellant). Air-breathing engines are necessarily combined or integrated with rocket engines to climb beyond the stratopause the atmosphere, as thin air contains virtually no oxygen.

TBCC (turbine-based combined cycle) and RBCC (rocket-based combined cycle) systems are being developed as such integrated propulsion systems, where TBCC typically comprises turbojet, ramjet, and rocket engines, while RBCC involves ramjet, scramjet, and rocket engines [90–92]. Examples of TBCC include Skylon by Reaction Engines and SR-72 by Lockheed Martin [77,93].

The flight path is constrained by dynamic pressure in structural consideration for launch vehicles whether powered by rockets or air-breathing engines. The latter are characterized by additional restrictions on dynamic pressure because thrust production for air-breathing engines in supersonic regimes crucially depends on the dynamic pressure to enable combustion as a result of aerodynamic and aerothermal interactions (*e.g.*, shock waves, boundary layers). Dynamic pressure can also have significant impact on the operation of the air intake, which requires a certain range of dynamic pressure to start and remain started.

The types of propulsion and propellants have considerable influence on the management and operation of the space vehicles in both pre-launch and launch phases. For instance, liquid propellants require cryogenic systems and often turbopumps, whereas solid propellants offer ease of handling but difficulty in throttle control during flight, thus requiring careful design and planning of the trajectory and propellant charge (grain) [14].

The performance inevitably deviates from the optimal at off-design altitudes due to over- or under-expansion for rocket engines equipped with fixed geometry nozzles, while adaptive nozzles such as plug, expansion-deflection, and aerospike nozzles can effectively compensate for the atmospheric density variation with altitude change [94].

Space access with air-breathing propulsion, on the other hand, features self-compensation for altitude owing to air-breathing nature and external expansion (*e.g.*, SERN scramjet configuration) [95], but thermal management plays a key role for the success of sustainable flight; TBCC for hypersonic operation essentially requires pre-cooling of incoming airflow, while RBCC requires effective wall cooling particularly for the combustor section [90,96].

4.1.2. Launch trajectory dynamics

The point mass dynamics of a launch vehicle traveling over a spherical rotating Earth can be described by the following set of 3 degree of freedom (3DOF) equations of motion [97]:

$$\dot{r} = V\sin\gamma \tag{1}$$

$$\dot{\theta} = \frac{V\cos\gamma\sin\psi}{r\cos\phi} \tag{2}$$

$$\dot{\phi} = \frac{V\cos\gamma\cos\psi}{r} \tag{3}$$

$$\dot{V} = T - D - g\sin\gamma + r\Omega^2\cos\phi(\sin\gamma\cos\phi - \sin\phi\sin\psi\cos\gamma) \tag{4}$$

$$\dot{\gamma} = \begin{bmatrix} (T\sin\alpha + L)\cos\sigma - g\cos\gamma + \frac{V^2\cos\gamma}{r} + \\ + \Omega\cos\phi(2V\sin\psi + \Omega r(\cos\gamma + \sin\gamma\sin\phi\cos\psi)) \end{bmatrix} \tag{5}$$

$$\dot{\psi} = \frac{1}{V}\begin{bmatrix} \frac{T\sin\alpha + L\sin\sigma}{\cos\gamma} + \frac{V^2\cos\gamma\sin\psi\tan\phi}{r} + \\ - 2\Omega V(\tan\gamma\cos\phi) + \frac{\Omega^2 r}{\cos\gamma}\sin\phi\cos\phi\sin\psi \end{bmatrix} \tag{6}$$

$$\dot{m} = -\frac{m\,T}{g\,I_{sp}} \tag{7}$$

where r is the radial distance from the Earth centre to the vehicle, V is the Earth-relative velocity, θ and ϕ are the geodetic longitude and latitude, respectively, α is the angle of attack (incident angle), γ is the flight-path angle, and ψ is the velocity heading (*track*) angle. g is the gravitational acceleration, and Ω is the Earth's self-rotation rate. σ is the bank angle (positive to the right). T is the thrust acceleration, I_{sp} is the specific impulse of the propulsion system and m is the vehicle mass. L and D are the lift and drag accelerations, respectively:

$$L = \frac{1}{2m}\rho V_R^2 S C_L(\alpha, Ma) \tag{8}$$

$$D = \frac{1}{2m}\rho V R^2 S C_D(\alpha, Ma) \tag{9}$$

Here ρ is the air density, S is the reference area, C_L, C_D are the lift and drag coefficients respectively and V_R is the velocity relative to the wind: $V_R = V - V_{wind}$. The dependency of the aerodynamic coefficients on the Mach number Ma is also highlighted.

4.1.3. Path constraints

Launch vehicles undergo steady acceleration by engine thrust to achieve the target final velocity ΔV requirement. In addition, they must endure instantaneous peak accelerations including mechanical shocks characterized by extremely high acceleration levels and high-frequency local loading with a duration in the order of milliseconds. The peak acceleration is higher for loss-mass payload launchers, while it is lower for larger launch vehicles [98]. Vibration and aeroacoustics can also have severe impact during launch, including peaks from rocket motor firing of main engines and turbopump operation for liquid propellants at lift-off, and aerodynamic buffeting due to unsteady flow motion in transonic flight [12,13].

Dynamic pressure is a crucial factor due to its potential impact on the vehicle structure especially when it peaks at a certain speed and altitude (as shown by the “Max Q” point in Fig. 1). It also plays a critical role in air-breathing propulsion systems, as described in Section 4.1.1, and needs to be maintained in a suitable range to enable efficient engine operation and avoid engine unstart, which can lead to a catastrophic failure. Aerothermal heating from skin friction and shock waves becomes significant at higher velocity in supersonic and hypersonic flight, necessitating appropriate thermal management accounting for heat transfer and materials [99]. The payload, which is often stored in the launch shroud where maximum temperature is reached, requires particular care against not only aerothermal and mechanical effects but also the pressure environment which steadily decreases with the altitude [14].

The constraints imposed on launch vehicles can be summarised as

follows:

$$n = \sqrt{L^2 + D^2} \leq n_{max} \tag{10}$$

$$q_{min} \leq q = \frac{1}{2}\rho V^2 \leq q_{max} \tag{11}$$

$$\dot{Q} = K_Q \rho^{0.5} V^{3.15} \leq \dot{Q}_{max} \tag{12}$$

where is the magnitude of L and D acceleration forces, q is dynamic pressure, ρ is atmospheric density, $\dot{Q}$ is the heating rate, and K_Q is a constant specific to spacecraft material.

To reduce the aerodynamic loads on the structure of a space launcher the first two constraints are often summarised by the following "q time alpha" constraint:

$$q\,\alpha < (q\,\alpha)_{max} \tag{13}$$

In fact $q\,\alpha$ is proportional to the aerodynamic load. This constraint is fulfilled during the first phase of the launch because the velocity V is low, then large α angles are allowed to rotate the launcher from its initial vertical attitude and implement the so called pitch manoeuvre. At "pitch over" the angle α becomes zero and it is kept very low during the atmospheric flight to guarantee the qα constraint. This constraint disappears during the ascent since the density of the air decreases exponentially with the altitude.

To maintain the angle α close to zero the local wind velocities V_{wind} are taken into account. Wind velocities are measured at different altitudes around the launch base till few minutes before the launch to update the nominal zero-lift trajectory (also called gravity turn trajectory). An ascending (safety) corridor is designed around the nominal trajectory: possible perturbations due to wind gusts and small model discrepancies as well as small hardware failures can produce moderate displacements from the nominal trajectory that can be recovered by the launcher control system. However if the launcher exits the ascending corridor a destruction command is actuated either by the Launch Officer, who tracks the trajectory on ground, or by the autonomous destruction system located on board. Namely, linear shaped charges are placed at the surface of the launcher case along the longitudinal axis. This arrangement limits the debris produced by the charge explosion: models of the mass and velocity distribution of the fragments are developed. For instance the velocity distribution of the fragments of the third stage of Ariane V is modelled by the formula:

$$D_V = rand(0,1)\, A\, m_F^{-B} \cdot \text{km/s} \tag{14}$$

where rand(0,1) are random numbers between 0 and 1 chosen according to a Gaussian distribution, m_F is the mass of the fragment (in kg) and A, B are the numbers: A = 0.2154, B = 0.1590. The mass of the fragment is related to its dimension d_F according to an empirical formula:

$$m_F = f\, d_F^G, \quad f = 45, \quad G = 2.26 \tag{15}$$

From this formula the ballistic coefficient of each fragment is estimated by:

$$B = \frac{1}{2} S\, C_D / m_F \tag{16}$$

with C_D ranging from 0.2 to 2. Considering different values of f ranging from 10 to 60, G ranging from 2.25 to 2.50, and the velocity variations D_V, the trajectories of the fragments are computed till the impact to the ground. All the possible values of altitude, velocity and flight path angles of the nominal trajectory are considered as initial state of the fragments, corresponding to all the possible points where the destruction command can be activated. In this way regions surrounding the nominal trajectory are computed: these regions must be avoided during the launch activity.

4.2. Re-entry

Historic catastrophic losses during re-entry procedures highlight the significant limitations imposed by physical phenomena such as aerothermal heating, dynamic pressure and structural loading. A future STM/ATM system will have to support both safe and unsegregated re-entry operations and accommodate the projected increase of de-orbiting LEO supply spacecraft among sub-orbital re-entry trajectories intended for global point-to-point transport operations. The following sections provide a concise outline of the evolution of common re-entry planning methods, highlighting the limiting features that will inevitably affect STM/ATM coordination.

4.2.1. Re-entry dynamics

The control of the re-entry capsule is provided by aerodynamic torque. This torque depends on several parameters and on two control variables: the incidence angle α and the bank angle σ. Incidence angle is changed by a rotation in the symmetry plane of the capsule (pitch rotation) and bank angle is changed by rolling the capsule around its longitudinal axis. To implement these rotations, different actuators are used corresponding to different re-entry capsule configurations. Ballistic capsules (having small aerodynamic efficiency C_L/C_D) generally use movable masses to change the static margin, which is the distance between the capsule centre of mass and the aerodynamic centre of pressure. This changes the stable attitude of the capsule, i.e., the value of α (α_{trim}) needed to ensure the flight in equilibrium condition. The bank angle can be changed by the rotation of the capsule around its longitudinal axis, generally implemented by cold gas jets generating a roll manoeuvre. On the other hand lifted re-entry capsules (high aerodynamic efficiency) are endowed with movable aerodynamic surfaces to control the capsule in pitch and roll.

4.2.2. Shuttle guidance concept

Since its publication, the Shuttle guidance and trajectory design developed by Harpold has been used as the baseline for the majority of research regarding the re-entry problem, and hence outlining the underlying principles will be instrumental to identify the progressions in re-entry design that followed. The primary objectives of the shuttle guidance are [100]:

1. To guide the orbiter along a path that minimizes the demands on the orbiter system design throughout the orbiter missions
2. To deliver the orbiter to a satisfactory energy state and vehicle altitude at the initiation of the terminal guidance system

During re-entry the above constraints limit the orbiters altitude at a given velocity, which can be expressed in terms of drag and acceleration. These constraints when visualized in a velocity/drag acceleration space produce what is known as a re-entry corridor. Fig. 4 demonstrates

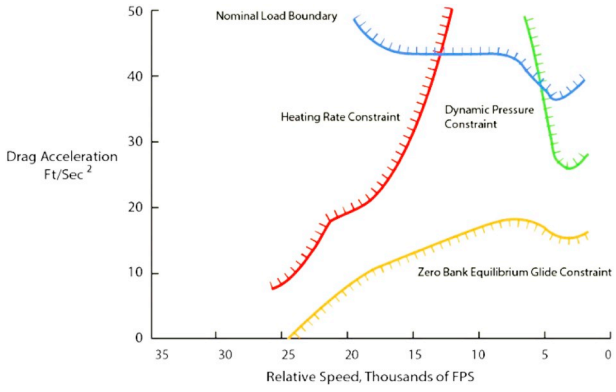

Fig. 4. Orbiter guidance corridor [100].

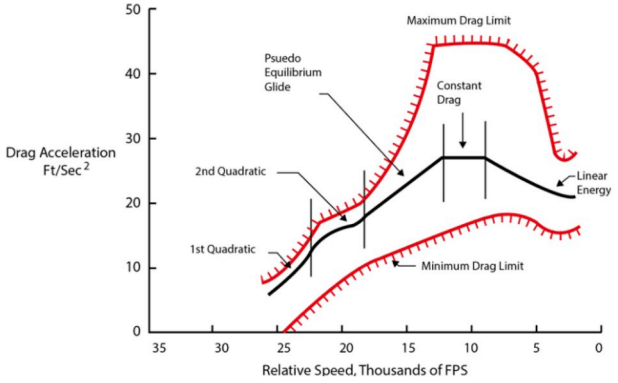

Fig. 5. Orbiter drag segments [100].

the bounds of the shuttle re-entry scenario.

The shuttle guidance entry concept assumes the hypersonic portion of the flight is considered a great circle arc extending from the initial entry interface to the terminal area energy management (TAEM) interface. Terminal and entry points are specified by a longitude, latitude, altitude above mean sea level (AMSL) and speed [20]. This assumption allows an initial estimate of the range to be flown (S_{togo}^{*}). A calculated guess of S_{togo}^{*} is an important parameter in designing the shuttle drag profile as the following will demonstrate. In constructing the appropriate drag profile the shuttle orbiter uses five drag reference segments. By connection of these segments a 2 dimensional "flight path" is then constructed from the entry interface to the terminal area.

Fig. 5 shows the five drag reference segments. The first 2 segments are a quadratic function of (r,V) and are used during the period of high heating on the orbiter, followed by a quasi-equilibrium glide (QEGC) and an linear energy segment. Note that these segments lie within the entry corridor, and therefore satisfy the given constraint. The use of the former two segments in re-entry guidance (QEGC, Energy) is extremely convenient and has been the subject of numerous studies on the matter. The use of these conditions are further discussed in 4.2.4 and 4.2.3.

The drag profile now acts as the reference drag acceleration profile, that is, the profile that the orbiter follows to match a desired speed at a given altitude. Further, each point on the reference profile can be described in terms of S_{togo}^{*} by means of solutions to the equations of motion. Under the QEGC condition Earth-relative speed is treated as the independent variable. The latter section of the where a strong monotonic drag profile is employed, energy is treated as the independent variable.

Understandably for the orbiter to achieve objective 2, S_{togo} calculated from the reference S_{togoD} must closely match the estimated S_{togo}^{*} otherwise the orbiter will not meet the desired terminal conditions.

To accommodate for deviations in the reference profile during re-entry phase, the magnitude of the drag profile is frequently updated so that $S_{togo}^{*} \approx S_{togoD}$ while maintaining the original reference shape to avoid any constraint breaches. For the orbiter to follow the constructed drag profiles, reference parameters are established to relate the lift and drag acceleration forces to each drag segment through the appropriate independent variable.

In following the desired reference profile, controllable inputs; bank angle σ, angle of attack α , are scheduled as function of the acceleration forces. Bank angle is chosen as the primary trajectory control parameter, where its magnitude dictates the total downrange while the sign of the bank angle commands the orbiter heading. An obvious consequence of a sustained bank will be heading deviation from the desired terminal interface, therefore a pre-defined heading error is set to schedule a reverse in the bank angle sign. Further, conducting a bank reversal requires the bank angle to roll through zero, directing the lift vector is upwards. A temporary increase in the in-plane component of lift results in a deviation from the desired drag level and introduces phugoid motion. To minimise these transient effects modulation of the angle of attack compensates for the brief period of deviation from the nominal drag profile.

The Shuttle guidance concept outlined above has proven extremely successful through flight tests and multiple shuttle missions and additional performance analysis [101], however it is subject to the main assumption of a 2 Dimensional Trajectory [20]. The relatively coarse lateral motion planning severely limits its applicability in achieving mixed TBO operations envisioned for a future ATM/STM system. Subsequent publications have focused on improving the Shuttle guidance's shortcomings while still retaining the attributes that made it highly effective. The following sections briefly recapture some of these successful approaches that have stemmed from the traditional Shuttle method.

4.2.3. Evolved Acceleration Guidance for Entry

Comparable to the linear energy drag segment in the Shuttle planning method, the Evolved Acceleration Guidance for Entry (EAGLE) method formulates the re-entry problem as a monotonically decreasing energy problem beginning at the re-entry interface and terminating at the TAEM point. Total Energy (E) is defined as the sum of kinetic and potential components:

$$E = \frac{1}{2}V^2 - \left(\frac{\mu}{r} - \frac{\mu}{r_s}\right) \tag{17}$$

where r_s is the radial distance from the planet surface to the spacecraft center of mass.

The five state variables described by the equations of motion (γ,θ φ, ψ, r_s/r) are then scheduled as a function of decreasing energy E through the velocity components found in each equation of motion. Subsequently, the reference variables used by the planning function (σ, α) are defined as normalized functions of energy $\hat{E}$.

$$\hat{E} = \frac{(E - E_i)}{(E_f - E_i)} \tag{18}$$

where E_i , E_f are the initial and desired final energy values respectively. By definition, $\hat{E} = 0$ at the entry interface and terminating at $\hat{E} = 1$ at the TAEM interface. Similar to the Shuttle method, EAGLE imposes the constraints described in 4.1.3 while also highlighting the importance that the trajectory and controls should maintain sufficient margins from the given hard constraints to allow for dispersions [20].

The fundamental extension of the Shuttle planning method is that EAGLE accounts for lateral motion of the spacecraft during re-entry. This is achieved by assuming the re-entry path to be taking place on the surface of a sphere as opposed to the planar assumption taken by the shuttle method [20]. Further, the equations of motion are simplified from 5th to 3rd order by the assumption that $\gamma = 0$ throughout the hypersonic portion of the flight. The advantage of eliminating vertical dynamics from the equation of motion lies in avoiding phugoid type behaviour due to fluctuations in the kinetic and potential energy terms as well decreasing algorithm computation time [21].

EAGLE breaks down the re-entry problem into the following sub-problems [20]:

1. estimate the trajectory length and obtain initial drag profile;
2. using the estimate of the drag profile, solve the trajectory curvature sub-problem;
3. based on the solution to the trajectory curvature sub-problem, adjust the trajectory length and resolve the trajectory length sub-problem and obtain a revised drag profile.

Sub-problem 1 is solved in a similar manner to the Shuttle guidance concept, where a drag profile extends from an initial value through to a final value, corresponding to a longitude, latitude, velocity and altitude. In contrast to the Shuttle planning method, all the segments of the

reference profile are represented by a function of monotonically decreasing energy [21]. Sub-problem 2 determines the curvature of the trajectory by calculating the lateral forces that occur as a consequence of following the drag profile. The magnitude and direction of these forces are extracted from the command history of bank and angle of attack modulation [21]. Once the curvature is known, the total length is then determined and then trajectory length (sub-problem 1) is updated. This process continues until the value of the estimated trajectory length (from entry to final point) converges with the extracted length of the 3 dimensional drag profile the re-entry planning problem is solved.

The objective of EAGLE was to develop a planning method that would be capable of achieving more aircraft like operations through an on-board planning system that allowed significant cross range entries as well the ability to accommodate abort scenarios. This added benefit of the EAGLE over the traditional shuttle method demonstrates its capability in a future STM system [21].

4.2.4. Quasi-equilibrium glide condition

The Quasi-Equilibrium Glide Condition (QEGC) has been the centrepiece of multiple research efforts regarding the re-entry planning problem. The following is a brief outline of the most well-known QEGC re-entry planning methods proposed and published by Shen and Lu [15–19].

4.2.4.1. QEGC concept. For a considerable portion of the re-entry trajectory, the flight path γ of a lifting body spacecraft is very small and therefore negligible in determining in spacecraft position and velocity. By ignoring the Earth's rotation and setting $\cos\gamma = 1$ and $\dot{\gamma} = 0$ the equation of motion describing the rate of change of flight-path angle is simplified to [102]:

$$0 = \mathrm{L}\cos\ \sigma - \mathrm{g} + \frac{\mathrm{V}^2}{\mathrm{r}} \tag{19}$$

The assumption of the QEGC is applicable to a given cut-off velocity where the magnitude of this velocity is dependent on the $\frac{L}{D}$ of the re-entry vehicle. For instance, a re-entry vehicle with $\frac{L}{D} \leq 1$ such as the X-33, X-38 the QEGC assumption is only valid $V \geq$ 2000 m/s, however for re-entry with $\frac{L}{D} \geq 1$ such as the Shuttle orbiter the QEGC provides a valid estimate of spacecraft position/velocity until a cut-off velocity associated with desired TAEM conditions condition [19]. On closer inspection of the QEGC condition, it is clear that any point on the re-entry trajectory where a distance r and velocity V is specified, σ will be adjusted to satisfy the QEG condition. Further, the QEGC allows a simple and effective way to construct the re-entry corridor within the velocity/altitude space if:

$$\sigma_{\mathrm{EQ}}(\mathrm{V}) \leq \sigma(\mathrm{V}) \leq \sigma_{\max}(\mathrm{V}) \tag{20}$$

Where if $\sigma_{\mathrm{EQ}}(\mathrm{V})$, $\sigma_{\max}(\mathrm{V})$ are chosen to satisfy the QEGC and the hard path constraints, the corresponding trajectory will satisfy all the imposed constraints [15]. Fig. 6 depicts the key characteristics of the QEGC.

4.2.4.2. QEGC algorithm. Shen (2002) [15] divides the re-entry trajectory into the following three distinct phases.

1. Initial Descent Phase
2. QEG Phase
3. Pre-TAEM Phase

The initial descent phase extends from the entry interface to an altitude where the QEG condition becomes valid (120 km - 80 km). Up until this point the QEGC is not an accurate estimate of the velocity and position of the vehicle as the lack of air density at higher altitudes does not provide sufficient dynamic pressure required for the generation of lift and subsequent trajectory controllability. Until the re-entry vehicle can satisfy the QEGC it is in somewhat of a controlled fall. During this phase a nominal angle of attack profile and constant bank angle are chosen to ensure a smooth transition to the QEGC phase. As discussed the QEGC phase is subject to all constraints and the length of its validity is determined from the magnitude of the re-entry vehicle's L/D. Depending on the bounds of the QEGC there may be no need assess phase 3. In the case of a re-entry vehicle with $\frac{L}{D} \leq 1$, the pre-TAEM phase is evaluated as a fourth-order polynomial of *(r,V),* a similar approach to the first phase of the shuttle entry scheme [15]. Fig. 7 presents the phases in the velocity/altitude space, while Fig. 8 presents the top-level QEGC.

Analogous to the EAGLE and shuttle methods, the point at which the bank reversal occurs is chosen to minimise the heading error at the TAEM interface. If the bank reversal is performed too early or late, the final heading error has the potential to be quite large. Once a suitable bank reversal point is located, the equations of motion are integrated to obtain a full 3DOF trajectory.

4.2.4.3. Suborbital Re-Entry planning. Suborbital re-entry differs from orbital in that the re-entry interface begins at significantly lower velocity and altitude in contrast to traditional re-entry procedures beginning from LEO. As a consequence the validity of re-entry trajectory generation methods based on the QEGC is questioned: if the spacecraft platform does not have an exceptionally high $\frac{L}{D}$ ratio the QEGC condition may not be satisfied due to the lower velocities associated with suborbital entry. Nevertheless, Shen and Lu proposed a method to extend the (r,V) polynomial from the TAEM interface to the end of the initial descent phase permitting suborbital trajectory generation for spacecraft platforms that exhibit lower $\frac{L}{D}$ ratios [16]. Future point-to-point spacecraft platforms associated with suborbital operations will most likely not succumb to the shortcomings associated with a low $\frac{L}{D}$ ratio as identified platforms are intended to operate tactically alongside traditional atmospheric aircraft.

4.2.4.4. Waypoints and No-Fly zones. The use of waypoints and geofences such as no-fly zones (NFZ) during re-entry will most likely be a cornerstone requirement for re-entering spacecraft achieving mixed operations with traditional atmospheric aircraft, as these relatively simple geometric entities provide a means to accurately constrain the re-entry trajectory. As discussed, traditional re-entry methods first design the longitudinal profile and then command the bank angle to follow the reference profile, where then the full 3DOF trajectory is obtained by integration of the equations of motion. This approach however is not appropriate when considering no fly zones and waypoints as lateral motion is an indirect function of the longitudinal planning and therefore may breach desired waypoints and geofences. Notwithstanding, re-entry planning methods have been proposed that simultaneously design the lateral and longitudinal motion to meet NFZ-like and waypoint constraints. However the proposed algorithms can take multiple minutes to produce a valid solution deeming it somewhat ineffective for online trajectory generation, a capability that will be required for tactical de-confliction scenarios in mixed flow TBO [103].

4.3. On-orbit phase

As spacecraft travel beyond the Earth's atmosphere, they become subject to an environment that is distinctly different from that on Earth. Space weather events generally shielded by the Earth's atmosphere now become hazardous. Aerodynamics surfaces become ineffective, requiring the use of non-air-breathing propulsive forces. Trajectories begin to follow initially somewhat deterministic ballistic and orbital paths however uncertainty in there prediction begins to grow due to the highly non-linear dynamics that govern the motion. This aspect becomes particularly problematic for long-term predictions required for separation assurance between other spacecraft (operational and defunct) and debris in the on-orbit environment. A future STM system

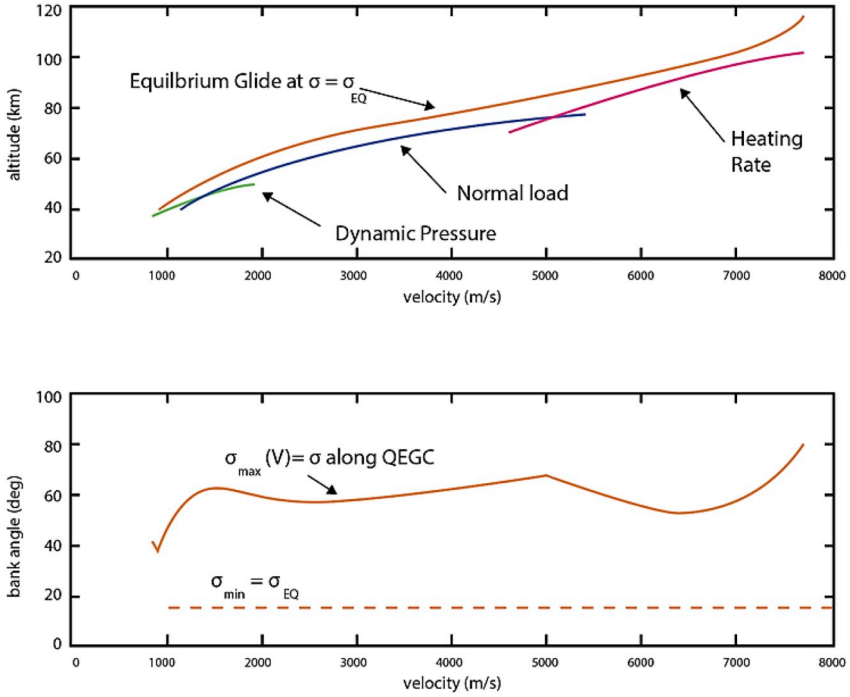

Fig. 6. QEGC: (a) Re-entry corridor; (b) Bank angle corresponding to path constraints [15].

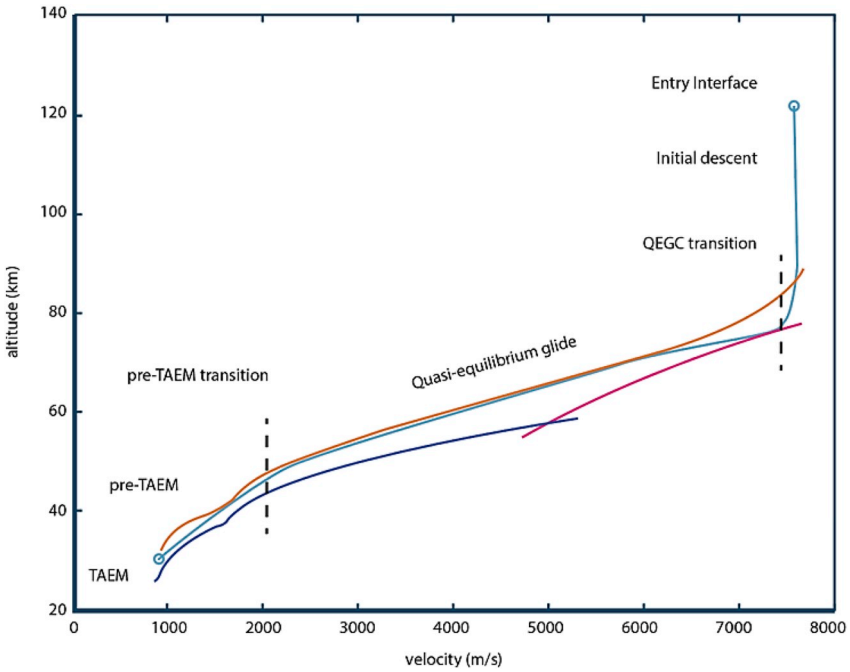

Fig. 7. Re-entry phases [15].

must fully consider these elements when developing operational procedures and decision support tools. Because of this, in the following sections we briefly summarise orbital dynamics modelling and subsequently review in detail the most relevant factors affecting the on-orbit phase and finally discuss how these can be captured when calculating long-term estimations.

4.3.1. Orbital dynamics

Cowell's method is a well-known deterministic approach for modelling orbital motion, for which the spacecraft trajectory can be estimated by a direct integration of the equations of motion including all relevant perturbations and propulsion accelerations. Historically, numerical solutions to Cowell's method had issues with accuracy due to the limited floating point precision in legacy computing technology; however advances in computing allowed this method to be a reliable, simplistic and accurate approach for orbital simulation.

The equations of motion for the two-body problem with initial conditions can be written as:

$$\ddot{\mathbf{r}} = -\frac{\mu}{r^3}\mathbf{r}\,(\mathbf{r},\ \dot{\mathbf{r}},\ t)\ t_0,\ \mathbf{r}_0,\ \dot{\mathbf{r}}_0 \tag{21}$$

where:

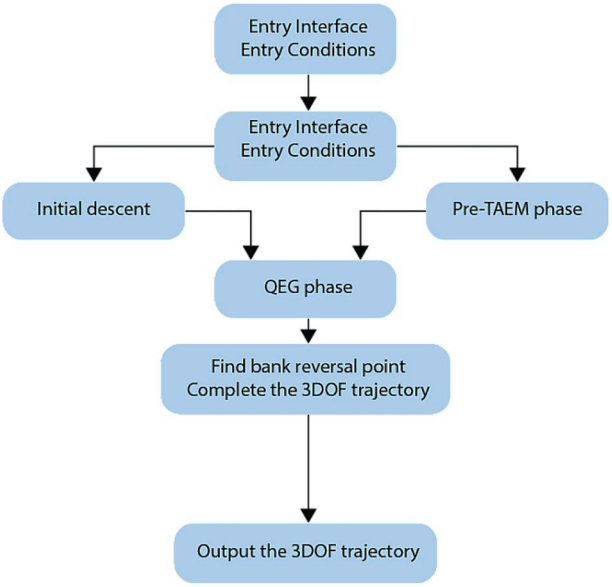

Fig. 8. QEGC algorithm [15].

$$r = \sqrt{x^2 + y^2 + z^2} \tag{22}$$

$$\mathbf{x} = \begin{Bmatrix} x \\ y \\ z \\ v_x \\ v_y \\ v_z \end{Bmatrix} \tag{23}$$

$$\dot{\mathbf{x}} = \begin{Bmatrix} v_x \\ v_y \\ v_z \\ \dot{v}_x \\ \dot{v}_y \\ \dot{v}_z \end{Bmatrix} = \begin{Bmatrix} v_x \\ v_y \\ v_z \\ -\frac{\mu}{r^3}x \\ -\frac{\mu}{r^3}y \\ -\frac{\mu}{r^3}z \end{Bmatrix} \tag{24}$$

$$\dot{\mathbf{x}} = f(\mathbf{x}, t) \tag{25}$$

4.3.2. Orbital perturbations

When predicting the short-term evolution of orbital motion in proximity of a relatively large gravitational attractor, the simplified two body problem is sufficient; however, when estimating long-term orbital evolutions, the effect of perturbations must be taken into account. Orbital perturbations in proximity of Earth can be classified in the three following categories [104]:

1. Perturbations due to the presence of other large celestial bodies and mainly:
   a. the Moon, $\mathbf{a}_m$
   b. the Sun, $\mathbf{a}_s$
2. Perturbations due to the Earth not being a perfect point-mass
   a. Oblate Earth (such as the J_2 term), U
3. Perturbations due to non-gravitational sources:
   a. Residual atmospheric drag, $\mathbf{a}_d$
   b. Solar radiation pressure $\mathbf{a}_{SRP}$

The total perturbation in proximity of Earth ($\mathbf{a}_p$) is then simply summed into the two-body problem using the Cowell formulation:

$$\mathbf{a}_p = \mathbf{a}_d + \mathbf{a}_s + \mathbf{a}_m + \mathbf{a}_{SRP} \tag{26}$$

$$\ddot{\mathbf{r}} = -\frac{\mu}{r^3}\mathbf{r}\, U + \mathbf{a}_p(\mathbf{r}, \dot{\mathbf{r}}, t) \tag{27}$$

The following sections provide the analytical expressions for these perturbations, expressed each as accelerations.

4.3.2.1. Non gravitational sources. The perturbing acceleration due to atmospheric drag is expressed as:

$$\mathbf{a}_d = -\frac{1}{2}\rho(\mathbf{r}, t)|\mathbf{v}_r|\mathbf{v}_r\frac{C_d A}{m} \tag{28}$$

where:

$\mathbf{v}_r$ = space object velocity vector relative to the atmosphere
ρ= atmospheric density
C_d = drag coefficient of the space object
A= reference area of the space object
m= mass of the space object

The relative velocity vector $\mathbf{v}_r$ is given by the space object velocity minus the cross product of the inertial rotation vector of the Earth's velocity, $\mathbf{w}$, and the position vector of the satellite, $\mathbf{r}$.

$$\mathbf{v}_r = \mathbf{v} - \mathbf{w} \times \mathbf{r} \tag{29}$$

$$\mathbf{w} = \omega_e[0\ 0\ 1]^T \tag{30}$$

$$\mathbf{v}_r = \begin{bmatrix} \mathbf{v}_z + \omega_e x \\ \mathbf{v}_y + \omega_e y \\ \mathbf{v}_z \end{bmatrix} \tag{31}$$

The solar radiation pressure constant can be expressed as:

$$C_{SRP} = \gamma P_s A_u{}^2 - \frac{A}{m} \tag{32}$$

where:

γ = reflectivity constant of the space object
P_s = solar radiation constant
A_u = astronomical unit
A = surface area normal to the incident radiation
m = mass of the space object

The acceleration vector due to solar radiation pressure is then given by:

$$\mathbf{a}_{SRP} = C_{SRP}\frac{\mathbf{r}_{b-s}}{|r_{b-s}|^3} \tag{33}$$

where:

$\mathbf{r}_{b-s} = \mathbf{r}_b - \mathbf{r}_{e-s}$
$\mathbf{r}_b$ = geocentric inertial position vector of space object
$\mathbf{r}_{e-s}$ = geocentric inertial position vector of the Sun

4.3.2.2. Non spherical Earth. The zonal perturbations given by the non-spherical Earth can be expressed as:

$$U = \left[1 - \sum_{n=2}^{\infty} J_n \left(\frac{R_E}{r_E}\right)^n P_n(\cos\theta)\right] \tag{34}$$

where:

r_E = distance from the Earth's centre
R_E = equatorial raduis of the Earth
θ= colatitude
J_n = zonal harmonic coefficient of the Earth of degree n
P_n = Legendre polynomial of degree n

Corresponding zonal harmonic coefficients and Legendre polynomials are outlined in Table 1.

4.3.2.3. Large celestial bodies. The perturbing acceleration from the

Table 1
Zonal harmonic coefficients and Legendre polynomials.

n	J_n	$P_n(\cos\theta)$
2	1082.63	$\frac{1}{2}(3\cos^2(\theta-1))$
3	−2.53215	$\frac{1}{2}\cos\theta(5\cos^2(\theta-3))$
4	−1.61099	$\frac{1}{8}(35\cos^4\theta-30\cos^2\theta+3)$

Moon can be expressed as:

$$\mathbf{a}_m = -\mu_m\left(\frac{\mathbf{r}_{m-b}}{|\mathbf{r}_{m-b}|^3}+\frac{\mathbf{r}_{e-m}}{|\mathbf{r}_{e-m}|^3}\right) \tag{35}$$

Where:

μ_m = Gravitational constant of the Moon
$\mathbf{r}_{m-b}$ = Position vector from the Moon to the space object
$\mathbf{r}_{e-m}$ = Position vector from the Earth to the Moon

Similarly, the perturbing acceleration from the Sun is given by:

$$\mathbf{a}_s = -\mu_s\left(\frac{\mathbf{r}_{s-b}}{|\mathbf{r}_{s-b}|^3}+\frac{\mathbf{r}_{e-s}}{|\mathbf{r}_{e-s}|^3}\right) \tag{36}$$

where:

μ_s = Gravitational constant of the Sun
$\mathbf{r}_{s-b}$ = Position vector from the Sun to the space object
$\mathbf{r}_{e-s}$ = Position vector from the Earth to the Sun

4.3.3. Space weather and other factors

The near-Earth space environment primarily comprises Earth's upper atmosphere, ionosphere, magnetosphere, and radiation belts, whereas deep space environment can include heliosphere and other planetary and small body regions in interplanetary space [25]. The near-Earth environment has crucial impact on the design and performance of space vehicles, which consistently operate in proximity to the Earth [14,25].

The Earth's atmosphere becomes thinner with altitude within the lower atmosphere ($h \lesssim 85$ km), where its pressure and density decrease exponentially, while maintaining a homogeneous composition mainly consisting of oxygen and nitrogen. In this altitude range, the pressure and viscous forces acting on the vehicle surfaces cause atmospheric drag to the spacecraft. Above this altitude, *i.e.*, thermosphere, which extends up to $h \lesssim 500$ km, the atmosphere becomes rarefied. The neutral atmosphere in the thermosphere is characterized by photoionization of molecules or atoms as well as absorption of UV photons radiated from the Sun, which leads to dissociation of molecules (constituent species of atmosphere are fully decoupled at $h \gtrsim 120$ km) [105]. The mean free path of the species becomes considerably large (significantly larger than the vehicle size at $h \gtrsim 180$ km), but their influence cannot be ignored. Cumulative effects of atomic and molecular impact on the vehicle and its orbit must be considered due to large kinetic energy associated with hypervelocity, as it represents a driving effect for altitude decay and associated along-track dispersions [106]. Density variations in the neutral thermosphere are linked with temperature variations in close relation to geomagnetic activities (*e.g.*, magnetospheric storms) and solar events, particularly solar winds with a 11-year cycle [106,107]. Reference [108] provides a comprehensive overview of approaches and modelling techniques available to estimate the drag encountered by space vehicles in the free molecular regime.

Plasma consisting of charged particles exists in the ionosphere at $h \gtrsim 85$ km (overlapping with the thermosphere), generated when neutral species are deprived of electrons by incident X-ray and photons from the Sun (photoionization), particularly on the dayside hemisphere. Energetic photons and electrons trapped in the Earth's magnetic field constitute the Van Allen radiation belt, presenting hazards such as degradation of spacecraft paints and protective glasses as well as surface temperature rise. Protons can cause greater damage due to larger mass hence momentum especially for LEO spacecraft operating in the South Atlantic Anomaly ($h \lesssim 500$ km). Electrons can trigger differential charging of spacecraft components, disrupting electronic components. High-energy electrons can penetrate the spacecraft and produce electrostatic discharges by bulk charging, disrupting subsystem signals and operation [109]. Such charge can subsequently harm electronic components in a form of single-event phenomena including single-event upset, latch-up, and burnout in a severe event [109,110]. Ionospheric plasma can also cause significant dispersion to electromagnetic radio waves by reflecting low-frequency waves, increasing propagation errors and thus causing inefficiencies in telecommunication systems [111]. Ionospheric disturbances and scintillations, in conjunction with geomagnetic storms, can subsequently have crucial impact on the GNSS performance, and thus requires the development of proper mitigation techniques, in consideration of uncertainties that remain in density irregularities of highly dynamic, strong ionospheric plasma [26–28].

Atomic oxygen results from photoionization of molecular oxygen by solar UV radiation in the atmosphere at $200 \lesssim h \lesssim 600$ km and becomes most predominant at $h \sim 200$ km due to gravitational influence, requiring particular consideration for the design and operation of LEO spacecraft. Solar arrays and sensor performance can be degraded irreversibly due to the interactions of atomic oxygen with materials such as composites, organic films, and metallized surfaces [112,113]. Outgassing (sublimation) of organic materials can occur when surface atoms are vaporized, subjected to very low ambient pressure, and they can represent a hazard to optically and electrically sensitive devices when deposited to the surface [114]. Space debris originating from various components such as spacecraft/instrument parts and rocket exhaust particles can cause severe damage to the space vehicles upon impact due to high kinetic energy carried by the objects, depending on the debris size and relative collision velocity [115].

The radiation environment associated with solar particle events and galactic cosmic radiation represents serious hazards against humans, necessitating appropriate shielding structures and materials for manned spaceflights [116,117]. Zero/microgravity environment can pose health risks in various aspects including blood pressure, muscular, locomotor and vestibular systems [14].

The near-Earth environment is thus characterized by both static and dynamic conditions (i.e., *space weather*), due to combined effects of atmosphere, thermosphere, magnetosphere, ionosphere, and gravity, in conjunction with the solar events, geomagnetic activities and other variations. Such conditions and phenomena can have crucial impact on space-borne and ground-based systems and also may endanger human health or life [110]. It is therefore essential to take the influence of space weather into account for space traffic management [22–24].

4.3.3.1. A case for space weather services as part of STM. When particularly referring to dynamic/unsteady phenomena, the term “space weather” is pertinent because these processes are hazardous to spaceflight in a manner not dissimilar to severe atmospheric weather phenomena such as thunderstorms, tropical depressions, icing, turbulence and windshear, which affect spacecraft during their atmospheric transits equally if not more substantially than aircraft. These severe weather phenomena can have safety-critical impacts on flight operations and are anyway cause of massive disruptions to operational regularity. These considerations equally apply to aircraft and spacecraft, with the added disadvantage that space vehicles are affected by both atmospheric and space weather. For instance, low-pressure systems and tropical revolving storms are known to cause significant disruptions to space launch and re-entry operations. Spacecraft operators rely on an increasing number of commercial

space weather providers for SSA due to the significant hazards and disruptions caused by nature on their operations.

On the other hand, weather forecast uncertainty is the single greatest challenge to denser 4D-TBO, as it can have opposite effects on inbound traffic from different directions, disrupting arrival sequences and/or compromising the scheduling and demand-to-capacity balance. Accurate and continuously updated weather information is therefore essential to mitigate perturbations in high-density 4D-TBO. This section briefly reviews the current aeronautical weather standards and planned evolutions before discussing the opportunity for STM to accommodate space weather information services.

The most relevant standards for Meteorological (MET) services are Radio Technical Commission for Aeronautics (RTCA) DO-308, 324 and 340, as well as the International Civil Aviation Organisation (ICAO) Annex 3. RTCA DO-340 specifies MET data link services in terms of service category, method of delivery and of the weather information involved [118]. Category 1 services are safety-critical and comprise both MET and Aeronautical Information Service (AIS) data links, whereas category 2 services are useful for decision support. In terms of timeframe and operational need, weather decision services are classified as either: Planning – supporting strategic long-range decision-making; Near-term – conceived for tactical avoidance of hazardous weather cells, particularly in terminal arrival/departure operations; and Immediate – supporting emergency avoidance and take-off/landing abortion. Longer timeframes correspond to larger geographic extents. All the services are supported by three delivery modes: Broadcast, which involve continuous regular transmissions to all aircraft within range, as opposed to Demand and Contract, which instead involve an active request for specific MET information. Table 2 illustrates the typical information provided by the three decision support services.

RTCA DO-324 specifies the Required Communication Performance (RCP) for MET service delivery in terms of Transaction Time (TT) [119]. Different TT requirements are defined for airport, terminal and en-route domains. RTCA DO-308, on the other hand, specifies the MET data formats: point data, area data, vector graphics and gridded data, and also identifies a list of candidate MET products [120]. Point data include, for example, the conventional Meteorological Aerodrome Report (METAR) and Terminal Aerodrome Forecast (TAF) – for which ICAO Annex 3 defines the recommended measurement and forecast accuracies [121] – as well as Snow Notice-To-Airmen (SNOWTAM), whereas examples of area data include Significant Meteorological Information (SIGMET). Gridded data consist in a 3D structured grid with a forecast time dimension.

ICAO's Aviation Systems Block Upgrade (ASBU) roadmap notably acknowledged that further improved meteorological services are required to implement advanced functionalities such as 4D-TBO, and indeed strategic planning services are already being supplemented by *nowcasting*, which uses sophisticated algorithms to track and extrapolate individual storm cells from weather surveillance sensors up to 6 hours into the future, with sub-kilometre spatial resolution and a temporal resolution in the order of minutes. Aviation weather service providers are increasingly supplementing this information with satellite imagery and ground-based sensors such as lightning detectors [122]. Some of these advanced weather services are already acknowledged by RTCA in DO-308, as shown in Table 3. The most recent standards also accommodate the capability of aircraft to downlink their locally-sensed weather information, which can augment ground-based data.

Drawing a parallel between STM and its atmospheric counterpart, it is important to note that ATM entail a number of AIS and MET services to accomplish its safety-critical air navigation mission, including for instance local winds and pressure dispatches, METAR, TAF, SNOWTAM as well as aircraft/pilot reports (AIREP/PIREP). More advanced ("*premium*") aeronautical weather information is instead available through non-ATM services and/or by subscription. These premium services are increasingly cherished by airlines as they allow to more effectively mitigate operational disruptions and to optimise flight routes. Although the current breakdown between basic (safety-critical) and premium aeronautical weather service categories, as captured by RTCA DO-340, was largely due to their historical evolution, it proves highly opportune when considering their different performance requirements. In particular, while fulfilling safety-critical requirements is feasible for basic weather services, it would prove inconvenient and unnecessary for premium services, which are increasingly based on sophisticate evolutionary and machine-intelligent-based forecast and extrapolation models to provide high resolution global coverage at all altitudes.

Whether the future STM system shall also cater atmospheric and space weather information services in a manner similar to ATM is certainly a worthwhile debate. While space weather-avoidance limitations of spacecraft may weight against such choice, essential orbital and sub-orbital estimations would be greatly benefited by a coordinated ground-based service. For instance, consistency in the 4DT planning and negotiation/validation processes and traffic synchronisation require consistency between the weather data in ground-based systems and the one handled by airborne/spaceborne systems as far as practical. This consideration strongly favours the introduction of a ground-based/centralised space weather service to support the functional air/ground integration being pursued as part of the CNS + A technological roadmap, which should be ideally extended to space. We suggest that by adopting or adapting the operational, level-of-service and timeframe categorisations introduced in RTCA DO-340 it would be easier to identify a baseline subset of information that could be delivered as part of the STM service.

4.3.4. Uncertainty in the orbital environment

The precise knowledge of a RSO's position and velocity is and will continue to be an increasingly important factor for the future air and space traffic management programs. These estimations are provided by cooperative and non-cooperative systems, most of which already fully accounted for as part of the CNS + A technological pathway. Cooperative systems rely on state estimates from on-board navigation systems (*e.g.* GNSS, IMU) and on their proactive exchange with all other vehicles in potential collision course, whereas non-cooperative surveillance is generally provided by tracking systems such as ground- and air-/space-based radar or electro-optical systems, which do not require response by the tracked object. These systems are subject to errors that are a function of physical phenomenon or from the mathematical extrapolation itself. Navigation and tracking errors are the differences between the measured states and the actual states of the space vehicle. Errors can particularly arise from either discrepancies within the reference coordinate system, from effects such as precession and polar motion or from errors specific to the position measurement such as clock accuracy, and atmospheric effects (ionospheric and tropospheric refraction) [29]. Tables 4–8 illustrate the performance of common spacecraft navigation and ground tracking related systems.

Table 2
MET information classified according to decision service [105].

MET Service	Planning	Near-term	Immediate
Time horizon	Greater than 20 min	3 min–20 min	Less than 3 min
Intended application	Offline and strategic online operations	Tactical online operations	Emergency avoidance, landing & take-off abortion
Airport Equivalent	METAR, TAF		Visibility, gusts and windshear

Table 3
Advanced METLINK products for flight planning in the USA and Europe [103].

	Data Format	Refresh Rate	Validity (hours)
US National Weather Service (NOAA)			
National Convective Weather Forecast (NCWF)	Gridded/Vector	5 min	1
Graphical Turbulence Guidance (GTG)	Gridded	15 min	0.25
Current Icing Product (CIP)	Gridded	1 h	N/A
Forecast Icing Potential (FIP)	Gridded	1 h	3
WIMS (FLYSAFE)			
WIMS thunderstorm	Gridded/Vector	5 min to 6 h	0.2–1
WIMS turbulence	Gridded/Vector	6 h	36
WIMS icing	Gridded/Vector	15 min to 12 h	0.24–24
WIMS wake vortex	Gridded/Vector	1–6 h	2–12

Representation of measurement errors is a key aspect in current orbital coordination and deconfliction operations, which is discussed in more detail in 5.4.2.

Commonly, the error in state vector measurements is expressed in the RSW satellite-based orbit coordinate system as shown in Fig. 9. The origin of the RSW of the coordinate system is located at the nominal position of the ECI state vector. The Radial (R axis) always points from the Earth centre along the radius vector towards the satellite. The S-Axis is directed in the along-track direction, where in the case of elliptical orbits is only parallel to the velocity vector at apogee and perigee. The W (cross-track) is normal to the orbital plane and completes the right-hand triad.

The RSW coordinate system can be easily related to the common adopted ECI coordinate system through the following unit vector transformation:

$$\hat{\boldsymbol{R}} = \frac{R_{ECI}}{|R_{ECI}|} \tag{37}$$

$$\hat{\boldsymbol{W}} = \frac{R_{ECI} \times V_{ECI}}{|R_{ECI} \times V_{ECI}|} \tag{38}$$

$$\hat{\boldsymbol{S}} = \hat{\boldsymbol{W}} \times \hat{\boldsymbol{R}} \tag{39}$$

The transfer matrix(s) between the RSW and ECI coordinate systems is the following:

$$M_{RSW \to ECI} = [\hat{\boldsymbol{R}}\ \hat{\boldsymbol{S}}\ \hat{\boldsymbol{W}}] \tag{40}$$

$$M_{RSW \to ECI} = [\hat{\boldsymbol{R}}\ \hat{\boldsymbol{S}}\ \hat{\boldsymbol{W}}]^T \tag{41}$$

Moreover, modelling errors occur from discrepancies in the orbital dynamic model. Errors included in the dynamic model are classified as the differences between the nominal model parameters and the real model parameters, which can be further categorised as rather gravitational or non-gravitational in nature. Typical gravitational parameters include: mass of the Earth, geopotential coefficients, solid Earth and ocean tide perturbations, mass and position of the Moon and planets, as well as general relativistic perturbations. Drag (due to atmospheric density), solar and Earth radiation pressure, magnetic perturbations and spacecraft thrusting (actuating errors) are the non-gravitational accelerations required for consideration in orbital modelling [29]. The general analytical expressions for these perturbations were provided in Section 4.3.2.

Table 5
Spaceborne inertial Sensor(s) performance [123].

Spaceborne Inertial Sensors	Accuracy	Limitations
Single-Axis Gyroscope (Fibre Optic, Ring Laser)	Angular random walk: 0.035–1 [μ rads / $\sqrt{s}$]	Subject to short and long term bias instability
Linear Accelerometer	20–400 μm/s^2	Subject to short and long term bias instability

Table 6
Reference spaceborne GNSS performance.

Spaceborne GNSS Sensors	Accuracy (3σ)		
GPS (GOES-R Spacecraft) [33]	Radial (R) 20 m	In-Track (S) 13 m	Cross-Track (W) 7.3 m

Table 7
Reference ground-based radar tracking accuracy.

Ground Based Radar Station	Accuracy (1σ)		
	Azimuth	Elevation	Range
AN/FPS 16 Single Object Tracking Radar [35]	0.1 mrad	0.1 mrad	5.4 m
AN/MPS 39 Multiple Object Tracking Radar [34]	0.2 mrad	0.2 mrad	2 m

Table 8
Ground-based optical tracking accuracy.

Ground Based Optical Station	Accuracy (1σ)		
	Azimuth	Elevation	Range
Super RADOTS Kwajalein Missile Range [124]	0.04 mrad	0.04 mrad	–
RADOTS Kwajalein Missile Range [124] [124]	0.07 mrad	0.07 mrad	–

Table 4
Spaceborne attitude sensor(s) performance [123].

Spaceborne Attitude Sensors	Accuracy [mrad]	Limitations	FoV [rad]
Sun Sensor	0.2–200		1 × 1
Earth Horizon Sensor	1–20	Accuracy is limited by the horizon uncertainty. Applicable to LEO spacecraft	(not applicable)
Star Tracker	0.005–0.30 (NEA)	Angular Rotation, Sun, Earth, and Moon stray light. Bias due to body frame misalignment.	≤ 0.45 × 0.45
Magnetometer	9–50	LEO Satellites, Accuracy is limited by the Earth's magnetic field uncertainty	(not applicable)

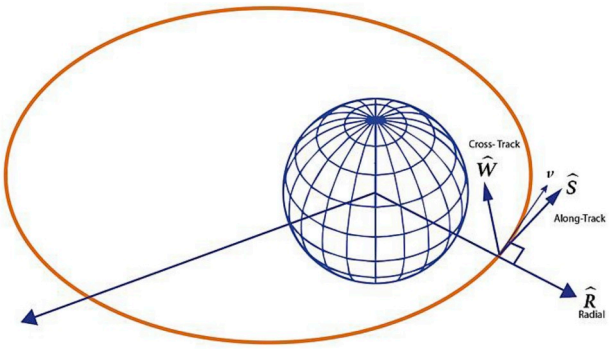

Fig. 9. RSW coordinate frame.

4.3.5. Orbital uncertainty propagation methods

Orbit propagation begins with an estimation of a space object's state vector. State measurement(s) are given by ground or on-board surveillance and navigation systems, for which measurement uncertainties can be assumed to be Gaussian and described by a mean and covariance matrix or PDF, unless otherwise recommended. From this initial state measurement, the orbit is propagated using one of the various approaches, inflating the position uncertainty ellipsoid with respect to time until the next measurement, which is commonly dictated by the update rate or availability of the navigation and/or surveillance system. The estimation of state can be seen as a convergent process that shrinks the volume of the ellipsoid at each observation epoch. Additionally, if any actuation is performed by the spacecraft the associated uncertainties should be included in the propagation at the time of manoeuvre [29].

An intuitive and rigorous empirical technique to propagate uncertainties and to reconstruct a statistical distribution is to perform the well-known Monte Carlo simulation, which involves the perturbation of initial states and of the dynamic coefficients in all their possible combinations. Nonetheless, conducting this approach with high fidelity is computationally expensive and can be deemed impractical in evaluating most collision scenarios.

A theoretical treatment of the stochastic uncertainty propagation in dynamic systems was attempted as early as 1914 and led to the Fokker-Plank Equation (FPE), which describe the evolution of the PDF in time for a problem that satisfies the Itô stochastic differential equation. This approach augments the original deterministic flight mechanics equations with statistical moments. Although extensive efforts were targeted at the development of a computationally efficient solution method for the FPE, the high dimensionality and the significant nonlinearities of rigid-body (6-DoF) orbital mechanics so far encumbered these efforts and forced to make extensive use of linearity and Gaussian statistics [125]. To overcome the challenges associated with the rigorous statistical treatment of nonlinearities and high-dimensionality, it is necessary to employ approximation methods. Lou and Yang [29] provide a comprehensive review on the available uncertainty propagation methods for spaceflight mechanics. Their ontology is recaptured in Fig. 10.

Of these, linear methods provide the user with a convenient approach as only the mean position and covariance matrix need to be propagated when the following assumptions are taken [29]:

1. A linearized model sufficiently approximates the dynamics of neighbouring trajectories with respect to a nominal trajectory
2. The uncertainty can be completely characterized by a Gaussian probability distribution.

The dynamics can then be linearized via local or statistical means under the well-known Linear Covariance analysis (LinCov) and CADET [126,127] techniques, respectively.

4.3.6. Unified sensor-centric approach

Considering the prospective certification requirements for non-segregated Unmanned Aircraft Systems (UAS) operations in all classes of airspace, an unified approach for multi-platform Separation Assurance (SA) and Sense and Avoid (SAA) was proposed [30]. This computationally inexpensive method allows to efficiently and effectively combine the measurement errors related to various navigation and tracking systems and to determine a combined avoidance volume that's position, shape, size and evolution can be computed in real-time [30].

The unified approach accounts for navigation and tracking measurements as well as relative dynamics and manoeuvrability and can adapt to both cooperative and non-cooperative encounters by considering the position, velocity and attitude uncertainties of both tracked and host platforms as well as their statistical correlation. A non-cooperative scenario in the orbital environment is defined as the encounter between a host spacecraft and space debris or potentially an uncooperative spacecraft (tracked by non-cooperative means), where only the host spacecraft has the ability to prevent a potential collision. Conversely, a cooperative scenario is defined as when all potentially colliding RSO have the means to exchange position information and when possible perform de-confliction manoeuvres. In the atmospheric context, SA&SAA capabilities for both cooperative and non-cooperative encounters are supported by a suite of forward looking sensors (active and passive), navigation systems (GNSS, IMU, vision-based), and cooperative surveillance systems (*e.g.*, ADS-B, ACAS-X).

Fig. 11 illustrates the combined avoidance volume calculated by statistically combining uncorrelated navigation and tracking errors. This sensor-centric approach has clear applicability to the orbital domain, where deconfliction processes have long relied on a simplified representation of measurement uncertainty.

5. STM framework and regulatory environment

The development of STM system will require the implementation of policy, rules and regulations, standards, guidelines and best practices. This task that will not be accomplished without significant legal and political barriers. In any case, policy related decisions will have significant influence on chosen technology and operational framework employed in a STM system. The technology domain acts to provide an STM system with Space Situational Awareness (SSA), which at a minimum, will enable an acceptable level of space-flight safety. This requires the necessary integration of products and services, applications, computing platforms, data sensors and other related technological aspects that together curtail the risks associated with existing and projected increase of orbital traffic. How these SSA related tools are controlled and maintained will be subject to the systematic steps, activities and actions defined within the operational domain. Evidently, the level of autonomy that will exist in executing these processes and procedures will be dictated by the complexity of required decisions and the effectiveness of Human Machine Interaction (HMI) within the operational environment. Decisions made within the policy domain shall capitalise on historical lessons, proven research, technical considerations, and operational limitations and time-lines [128] (Fig. 12).

The *outer space treaty* developed by the United States, United Kingdom, and the Soviet Union provides the basis of an STM framework. Comprised of 17 articles, the treaty addresses fundamental concerns including; the non-ownership of orbits and appropriation of space (Articles I, II), operator responsibilities in situations of distress (Article V) and damage liabilities from in space accidents (Article VII) among others. Although foundational, the Outer Space Treaty at present does not provide the necessary framework to assign space traffic management functions to new international decision-making STM authorities [129]. To accommodate such an aspect, it has been recommended that the treaty should be amended to establish a standing international organisation for STM, equivalent to ICAO and related atmospheric traffic standards and services [129]. Nevertheless, fast-forward 50 years and

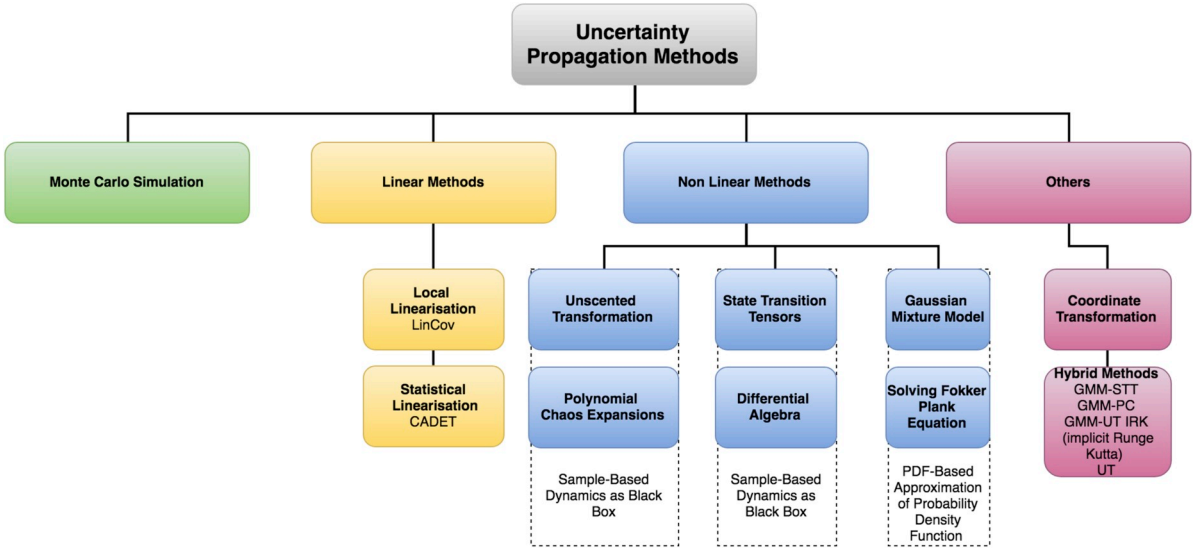

Fig. 10. Ontology of uncertainty propagation methods, reproduced from Ref. [29].

the problematic scenarios associated with the absence of a central STM authority are now becoming increasingly tangible.

In the interest of mitigating such events, many international and national organisations have developed various operational strategies, recommendations and requirements in the form of published guidelines and standards. The information contained in these documents address the specific hazard(s) present during each operational phase (launch, re-entry, on-orbit). The launch and re-entry phases are principally concerned with range safety which is addressed by Standard 321-07 “Common Risk Criteria Standards for National Test Ranges”. Standard 321-07 also extends to the on-orbit environment where separation and collision probability requirements are provided. Moreover, the on-orbit phase is subject to the irrefutably hazardous space-debris environment, with increasing concerns of initiating a irreversible, cascading debris generating process widely recognised as Kessler syndrome [39,40]. In consideration of the hazards imposed by space debris, mitigation guidelines and strategies have been issued by the IADC (Inter-Agency Space Debris Coordination Committee). The growth of space-based infrastructure has also introduced a different type of congestion - the frequency spectrum. As such the International Telecommunication Union (ITU) has developed a regulatory framework to mitigate frequency interference between spacecraft operating in the on-orbit environment. The following sections review these guidelines that form the basis of STM operational procedures.

5.1. Space Debris Mitigation Guidelines

Founded on the common findings and recommendations produced by several international and national agencies such as NASA, DLR, JAXA, ESA, AIAA, the IADC “Space Debris Mitigation Guidelines” have been developed as a comprehensive reference on recommended orbital debris mitigation strategies [31]. Focusing specifically on the following aspects, the IADC aims to provide guidance across all operational phases within the orbital environment.

1. limitation of debris released during normal operations;
2. minimisation of the potential for on-orbit break-ups;
3. post-mission disposal;
4. prevention of on-orbit collisions.

whereby spacecraft operation is comprised of the following phases (as defined by IADC):

Launch Phase *"Begins when the launch vehicle is no longer in physical contact with equipment and ground installations that made its preparation*

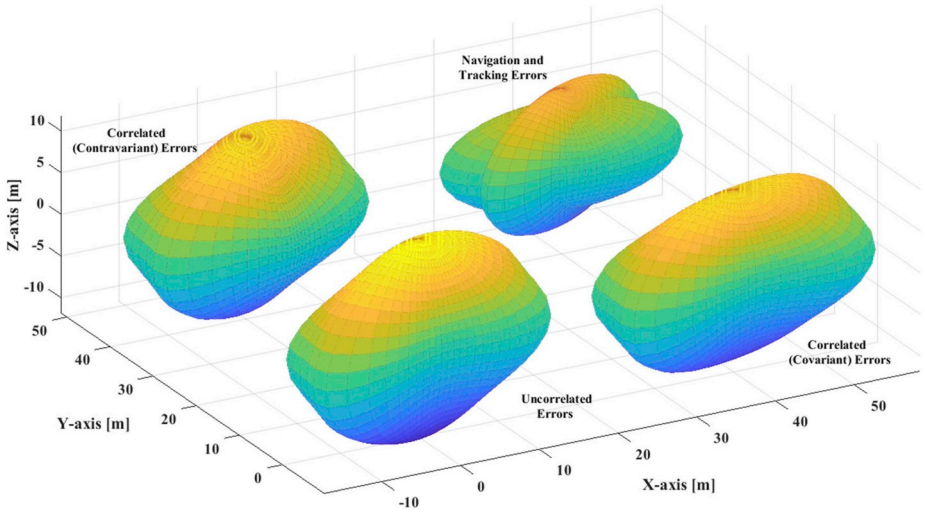

Fig. 11. Sensor-centric approach to position uncertainty.

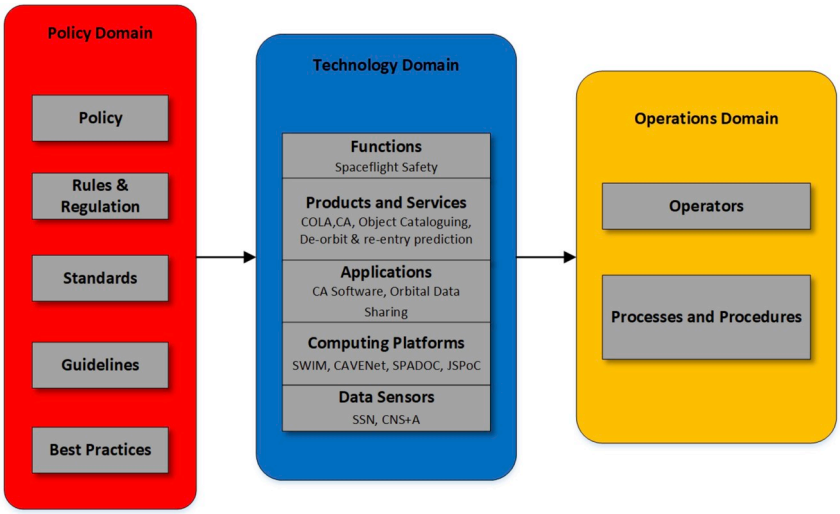

Fig. 12. STM framework. Adapted from [128].

and ignition possible (or when the launch vehicle is dropped from the carrier-aircraft, if any), and continues up to the end of the mission assigned to the launch vehicle."

Mission Phase *"The phase where the spacecraft or orbital stage fulfils its mission. Begins at the end of the launch phase and ends at the beginning of the disposal phase"*

Disposal Phase *" Begins at the end of the mission phase for a spacecraft or orbital stage and ends when the space system has performed the action to reduce the hazards it poses to other spacecraft and orbital stages"*

Additionally, guidelines are also provided in regards to the End of Mission/life phase, detailing relevant pacification measures that a spacecraft shall perform after its "useful" life. Fig. 13 illustrates the IADC framework, highlighting common causes of orbital debris and recommended mitigation practices across both operational and end of mission phases. Distinction is also made between the typical categories of space debris associated with different causes. Mission-related debris, fragments and spacecraft/rocket bodies are designated yellow, red and green respectively. Table 9 provides some examples associated with each debris category.

5.1.1. Protected orbital regions

Certain orbital regimes provide unique opportunities to conduct

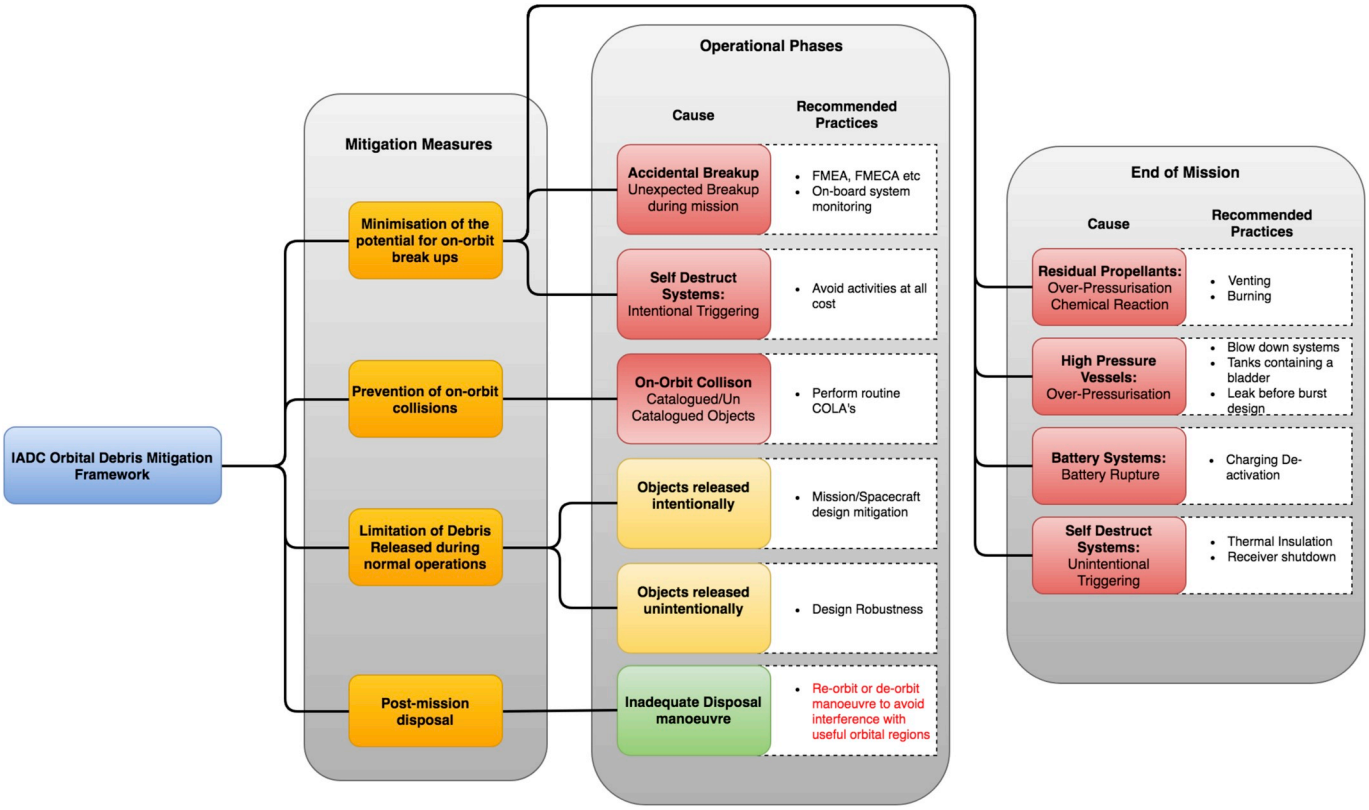

Fig. 13. IADC orbital debris mitigation framework.

Table 9
IADC Space debris categories, common causes and examples [130].

Main Categories	Causes		Examples
Mission-Related Objects	Objects released intentionally	General Operation	Fasteners, covers, wires
		Experimental	Needles, balls, Tethers cut after experiments
	Objects released Unintentionally	General Operation	Tether systems cut by debris or meteoroids, Objects released before retrieval to ensure safety, Liquids, Solid motor particles
On-Orbit Break Ups	Intentional destruction	Scientific/Military Experiments	Debris fragments
		Prior to re-entry (Minimise ground casualty)	
		Security Assurance of on-board devices	
	Accidental Breakup	During Mission	Debris Fragments
		Post-Mission	
	On-Orbit Collison	Catalogued/Uncatalogued Objects	Debris Fragments
Mission-terminated systems	Incorrect/Not-actioned disposal manoeuvre		Spacecraft and rocket bodies

Table 10
Protected orbital regions as defined by IADC.

Region	Description
Region A: Low Earth Orbit	Spherical region that extends from the Earth's surface up to an altitude of 2000 km
Region B: Geosynchronous Region	A segment of the spherical shell defined by the following: Altitude Bounds = Geostationary altitude (Z_{GEO}) ± 200 km within $-15^{\circ} \leq$ latitude $\leq +15^{\circ}$ $Z_{GEO} = 35786$ km

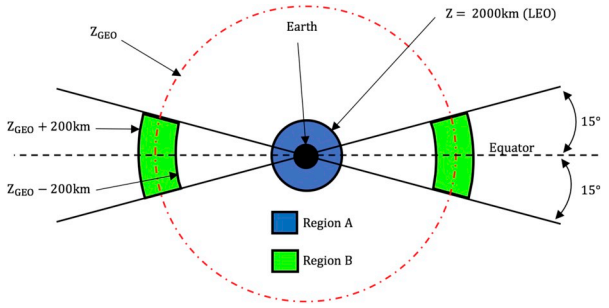

Fig. 14. Overview of LEO and GEO protected regions as per IADC [130].

specific operational applications. As such the number of RSO under GEO and LEO regimes continues to grow rapidly due to their distinct advantage in providing global communication, navigation, scientific and surveillance services. While a detailed discussion regarding the GEO regime is beyond the scope of this paper due to its limited relevance for space transport applications, some key aspects including the debris mitigation provisions developed by IADC are worthy of consideration. Understandably, maintaining the useful life of both of these regions is of high priority to ensure acceptable levels of safety for space operations and the sustainability of critical global CNS infrastructure. In doing so, the IADC has designated LEO and GEO protected regions in regards to the generation of space debris. Protected zones provide a basis for post-mission disposal operations and therefore are an inseparable component of a future STM system. Table 10 provides spatial description of the IADC defined LEO (A) and GEO (B) protected regions which are then shown graphically in Fig. 14. In contrast, a protected Medium Earth Orbit (MEO) region has not yet been warranted due to its low spatial density and rare use as a disposal zone. Nevertheless, it is recommended that where possible MEO operators should take a collaborative approach to mitigate the generation of space debris [131]. The following sections outline the recommended disposal strategies for spacecraft operating within the LEO and GEO regions.

5.1.1.1. Geosynchronous disposal guidelines. The IADC states the following for mission-terminated spacecraft operating in the GEO protected region [31]:

> *"Spacecraft that have terminated their mission should be manoeuvred far enough away from GEO so as not to cause interference with spacecraft or orbital stage still in geostationary orbit. The manoeuvre should place the spacecraft in an orbit that remains above the GEO protected region."*

Studies conducted by the IADC have found effective post mission GEO disposal manoeuvres can be conducted by fulfilling two specific conditions [31]. The first of these conditions is a minimum increase in perigee altitude of:

$$235 \text{ km} + \left(1000 \cdot C_{SRP} \cdot \frac{A}{m}\right) \tag{42}$$

where 235 km corresponds to the sum of the upper altitude of the GEO protected region (200 km) and the compensation required for altitude reduction due to luni-solar and geopotential perturbations (35 km). C_{SRP} , $\frac{A}{m}$ is the solar radiation pressure coefficient and aspect area to dry mass ratio respectively. The second condition is a re-orbit eccentricity that satisfies the following:

1 An eccentricity ≤ 0.003, or
2. An eccentricity vector that is pointed so that the longitude of periapsis, ϖ, is pointed towards the winter or summer solstice. i.e.

$$\varpi = \omega + \Omega \approx 90^{\circ} \text{ or } 270^{\circ} \tag{43}$$

where ω is the argument of periapsis and Ω is the longitude of the ascending node. The implementation of these requirements will result in the space vehicle not re-entering into the protected zone over a 40-year period. Under the assumption that a spacecraft meets the minimum perigee altitude (condition 1), the graph shows that an operator may need only to consider the direction of the vector if the value of eccentricity (of the re-orbit) is above the prescribed value of 0.003. In the case of small eccentricities the IADC states that a smaller increase in perigee may be chosen if a sun-pointing vector is chosen due to the diminishing effect solar radiation pressure will have on perigee height variation. Nevertheless, the IADC states that for all re-orbit strategies it is highly advantageous to carry out further simulation studies to assess manoeuvre suitability. This is especially the case when eccentricity values > 0.003 are chosen due to the increased sensitivity between pointing angle and successful post mission disposal as illustrated by Fig. 15.

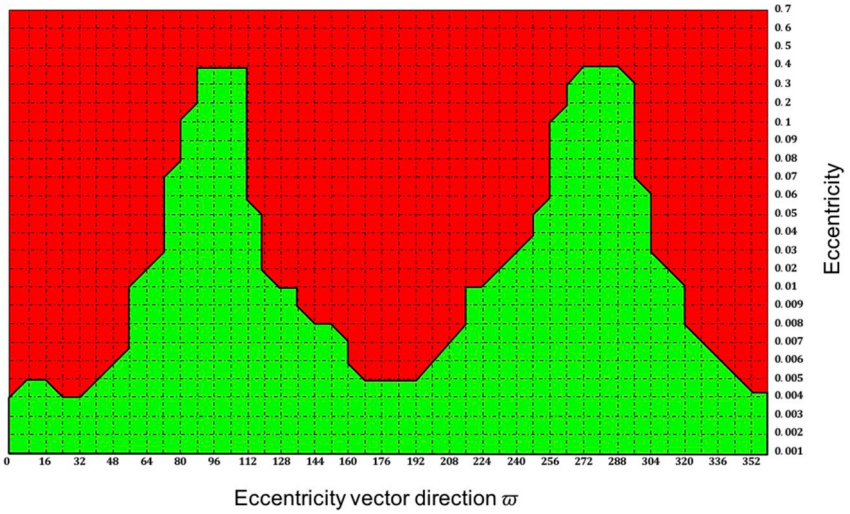

Fig. 15. Combinations of Eccentricity Vector directions and Values that will cause spacecraft to re-enter GEO protected zones (red) [130]. (For interpretation of the references to colour in this figure legend, the reader is referred to the Web version of this article.)

5.1.1.2. LEO disposal guidelines. With the aim of maintaining a balance between increased collision risk associated with extended post mission life and the substantial costs associated with reducing it, the IADC recommends the following guideline:

Post mission lifetime should be limited to 25 years for any spacecraft that passes through or has the potential to interfere with the LEO region.

Although direct post mission re-entry would be the most effective method in reducing LEO traffic and satisfying the above, it is by far the least efficient as it imposes a significant weight fraction penalty on spacecraft mission design. As such the exploitation of natural orbital perturbations is suggested as the primary mechanism to enforce eventual re-entry and ideally complete burnup.

Clearly, adhering to the 25-year policy requires post-mission disposal to be fully considered in mission and spacecraft design, most notably the propellant mass fraction associated with required manoeuvres. Inversely proportional to altitude, the effectiveness of atmospheric drag to decay a space object's orbit primarily depends on the final perigee of the spacecraft (after post-mission manoeuvre) and as such spacecraft operating in the outer periphery of the LEO region are imposed with heavier propellant weight penalties. Table 11 demonstrates this effect. For spacecraft that do not have the capability to perform de-orbit manoeuvres, the IADC recommends the following:

> "Satellites without de-orbiting capability should not be launched to the orbits within the LEO protected region if their post mission lifetime is greater than 25 years"

Obviously, by decreasing the altitude of post-mission spacecraft a congestion in the lower altitudes of the LEO region will eventually occur. Historically this region has been populated by manned spacecraft missions, a trend that is set to grow with envisioned commercial spaceflight operations. Nonetheless, the IADC guidelines state that the collision risk associated with an increasing population of disposed spacecraft is unjustified considering current tracking and collision avoidance capabilities within the LEO region [130].

Table 11
Propellant requirements for 25 year LEO post mission lifetime, reproduced from Ref. [130]. I_{SP} = 200 s, A/m = 0.05 m^2/kg.

Initial Circular Orbit Altitude	Final Perigee Altitude	Delta Velocity	Mass Fraction (propellant/dry mass)
800 km	730 km	18 m/s	0.8%
1000 km	630 km	88 m/s	4.3%
1500 km	535 km	236 m/s	11%
2000 km	495 km	349 m/s	17%

5.1.1.3. Post-Mission disposal compliance. Building upon the IADC guidelines, a suite of new space debris focussed standards have been published by the International Organisation for Standardisation (ISO) [32]. Consequently, identifying operational compliance of these standards is becoming an increasingly important topic of research. In particular this research focuses on monitoring LEO & GEO operational lifecycle trends as these actions can be observed somewhat conclusively through publicly available surveillance data.

While IADC protection region compliance is encouraging for the GEO regime, studies shown that compliance to IADC guidelines is still very low in the LEO regime, which includes the most relevant orbits for future space transport operations. In particular, findings from studies conducted by NASA (2012) [41] indicate a strong trend towards operational compliance of IADC guidelines with approximately 80% of end-of-mission spacecraft manoeuvring into GEO disposal orbits over the 2001–2010 period. Moreover, a 2014 ESA/European Space Operation Centre (ESOC) study [42] reaffirms these findings identifying that only approximately 10% of spacecraft are left abandoned, and 2/3 of disposal manoeuvres that are conducted are in full compliance of IADC guidelines. Nonetheless, there has been a shift towards the use of inclined GEO orbits due to the reduced propellant requirement associated with East-West station keeping [41], introducing higher relative velocities and subsequently an increased collision probability [132]. Additionally, highly inclined spacecraft such as the Chinese Beidou (55°) and U.S Sirius, (65°) operate a significant portion of their mission well outside the currently designated GEO protected regions.

In contrast, IADC compliance in the LEO region is more concerning. A 2014 study conducted by ESA [42] found that less than 50% of end-of-life (EOL) spacecraft (post-mission) *without* active de-orbit capabilities were under an orbital regime that would naturally decay within 25 years. Similarly, less than 50% of spacecraft *with* active de-orbit capability meet the post-mission lifetime criteria through either active or natural deorbit means. Upper stages left In LEO are the most compliant with approximately 75% meeting the 25 year criteria. In all cases natural decay due from orbital perturbations was identified as by far the most common mechanism in meeting the 25 year criteria. Nevertheless, when considering the densely occupied areas between 800 and 1100 km altitude, successful implementation of the 25 year strategy cannot solely rely on natural perturbations. As such the study recommends that considerably more effort is required from future EOL spacecraft residing within higher LEO altitudes to perform post-mission disposal manoeuvres to ensure operational sustainability of the LEO

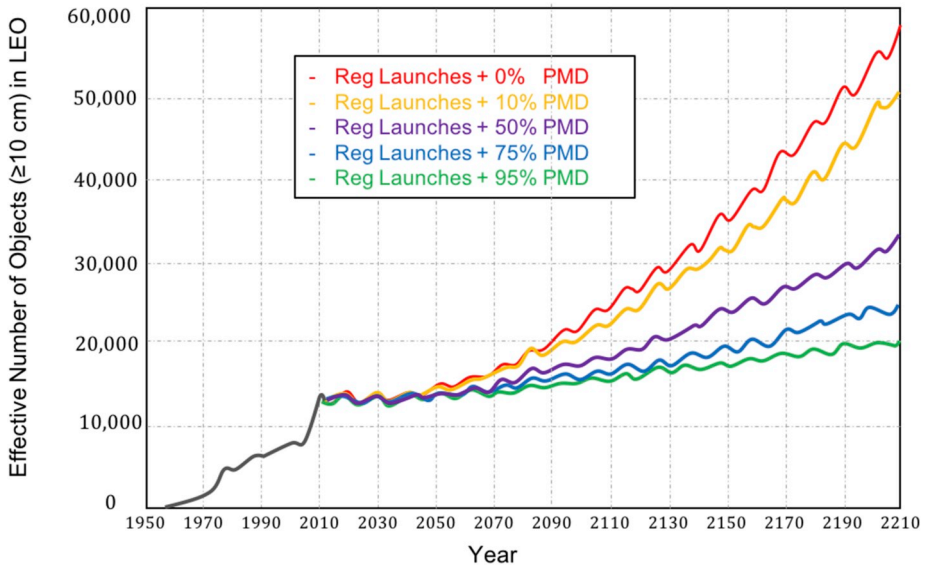

Fig. 16. Predicted LEO orbital debris evolution at various PMD compliance levels [43].

region [42].

Providing an updated view of the IADC guidelines first formulated in the 1990's, a study undertaken by NASA in 2013 [43] also highlights concerns with the LEO operational environment. Using predictive analytics in the form of Monte Carlo simulations of NASA's state-of-the-art orbital debris evolutionary tool LEGEND (LEO-to-GEO ENvironment Debris model), the study aims to identify the growth of the LEO population under varying levels of IADC 25 year post-mission disposal (PMD) compliance (Fig. 16). When considering the case of 95% PMD compliance, the study found that the average LEO debris population increase is limited to 54% over a 200 year period, with a collision occurring on average every 4.4 years [43]. However, when bearing in mind PMD compliance values reported by recent studies [42], 50% provides a realistic, if not, the best case representation of current operational compliance. Under this assumption debris growth rate is estimated at an alarming rate of 150% over the next 200 years with collisions occurring every 2.6 years. The results from this study highlight two critical points. Firstly, PMD can be an effective tool in reducing the growth of orbital debris, if and only if there is a dramatic shift towards increased operational compliance levels. Secondly, current PMD operations can only reduce the growth rate of LEO debris, whereas the total number would still increase in most scenarios, calling for novel active debris removal techniques to be urgently developed targeting the LEO environment [43].

5.2. International Telecommunication Union

The ITU is a specialised agency of the United Nations that is responsible for issues that concern information and communication technology. In the space domain, ITU is responsible for preserving the operational sustainability of satellite based communication infrastructure. As described by the ITU, “radiofrequencies and orbital slots are limited natural resources that must be used rationally, efficiently and economically”. In favour of interference free orbital slots and radio frequencies the ITU has developed a complex framework to promote safe and secure satellite operations. All civilian spacecraft are required to be registered with the ITU which is achieved through either a “first come – first served” or an “a priori” scheme [133]. In the former case, a request is made by the spacecraft operator that outlines the volume of orbit and spectrum resources required to satisfy their *actual* operational requirements [134]. Allocation and coordination of spacecraft orbit/spectrum activities are then performed with the aim of efficient integration into the current orbital environment. Alternatively, the “a priori” approach is intended at optimising *planned* orbital position and frequency allotment to reduce future congestion most commonly in the GEO region. The reservation of orbit/spectrum resources also ensures “equitable access” to all countries. This approach is particularly significant for developing countries that currently do not have the means to exploit space based assets [134].

5.3. Common Risk Criteria for National Test Ranges

With 1% of probability of fatality per flight [135], spaceflight has shown to be an inherently dangerous undertaking. This risk does not only apply to the people aboard the spacecraft, but to the general public also, with one quarter of all failures occurring during the first stages of operation [136]. To curb the risk associated with space flight, Standard 321-07, “Common Risk Criteria Standards for National Test Ranges” provided by the Range Commanders Council outlines the requirements and guidelines to provide adequate levels of safety during all flight phases, and as such is treated by the US Federal Aviation Administration (FAA) as the principal resource for space flight operation risk management [137]. The following section provides a top level description of important definitions and the risk management criteria outlined in Standard 321-07 [33–35].

Standard 321-07 identifies the following “at risk” categories during space vehicle operations:

1. manned spacecraft
2. active satellites
3. general public
4. non-mission aircraft criteria
5. mission-essential aircraft
6. non-mission ship

Each category is assigned an allowable level of “risk”, expressed in terms of individual probability of: individual casualty or fatality (general public), collision (manned spacecraft and active satellites), or impact (non-mission and mission-essential aircraft and ships) occurring for any single mission (Table 12).

Excluding manned spacecraft and active satellite categories, the maximum acceptable risk associated with the undesired event is fundamentally based on debris field dispersion – simply, the probability of casualties and or fatalities from debris due to the spacecraft undergoing a planned or unplanned catastrophic failure at any point in the mission.

Understandably, to quantify this risk, additional assessments must

Table 12
Standard 321-07 risk criteria.

Category	Max Acceptable	Undesired Event
1. Manned Spacecraft	1E-7	Individual Probability of Collision
	Ellipsoidal Miss Distance of 200 km in track and 50 × 50 km Cross Track and Radial	
	Spherical Miss Distance 200 km	Collision
2. Active Satellites	1E-4	Individual Probability of Collision
	Ellipsoidal Miss Distance of 25 km in track and 7 × 7km Cross Track and Radial	Collision
	Spherical Miss Distance 25 km	Collision
3. General Public	1E-6	Individual Probability of Casualty
	1E-7	Individual Probability of Fatality
4. Non-Mission Aircraft	1E-7	Probability of Impact
5. Mission-Ess. Aircraft	1E-6	Probability of Impact
6. Non-Mission Ship	1E-5	Probability of Impact

be carried out. These include (but not limited to) modelling space vehicle breakup, debris distribution, and impact probability within the atmospheric environment (as discussed in 4.1.3). In contrast, the undesired events associated with manned spacecraft and active satellites are aimed at reducing the risk within the orbital environment. Similarly, manned spacecraft (including those on route too or in support of manned missions) and active satellites are bound by “miss-distances" as well and the maximum probability of impact of 1E-7 with any other spacecraft or orbital debris 1 mm or greater [33–35]. Hence, accurate orbital insertion and comprehensive situational awareness of the space environment is crucial in conforming to the acceptable limits.

The Risk Criteria specified in Table 12 is calculated on a “per mission” basis, i.e., total risk over all flight phases, naturally imposing highly stringent requirements on the space vehicle. However, if certain conditions are met, separate risk budgets can be applied to each phase of flight. To explore this concept further it is necessary to outline the following definitions [34]:

Beginning of Flight *"Flight begins at a time in which a launch vehicle normally or inadvertently lifts off from a launch platform. Lift-off occurs with any motion of the launch vehicle with respect to the launch platform*".

Beginning of Mission Risks *"The beginning of mission risks may not always start at the beginning of flight phases, depending on the nature of the spacecraft*".

End of Flight for Expendable Launch Systems *"ELV end of flight occurs when orbital insertion is completed. Orbital insertion takes place when a launch vehicle achieves an orbital state or when its drag corrected instantaneous impact point leaves the Earth without intending to re-establish on the Earth prior to entry, and thrust has been discontinued*".

End of Flight Involving Re-entry *“RLV end of flight commences at the point of payload deployment, thus ending the "launch phase" of the RLV mission. Re-entry is defined as the event occurring when a spacecraft or other object comes back into the sensible atmosphere after going to higher altitudes, or the actions involved in this event*".

If a “decision point” exists between each distinct phase of flight, and where all the following conditions are met, separate risk budgets can be applied for each phase of flight:

1. The Vehicle has sufficient controllability to allow operational options that could reduce the risk posed by a subsequent phase (or phases) significantly.
2. The decision as to whether or how to proceed with a subsequent phase is based on a risk assessment that is conducted or validated just prior to each phase of flight.
3. The risk assessment for subsequent phases is made or validated using updated vehicle status and updated predictions of flight conditions

Nonetheless, a risk assessment undertaken previously can be considered valid if the assumptions made closely follow the current conditions of the mission. Further, the use of separate risk budgets is increasingly legitimate if the various flight phases pose hazards to distinctly different population groups [34].

5.4. Meeting space vehicle operation-risk criteria

Understandably, meeting the requirements associated with the various “at risk” categories mandates the implementation of phase specific procedures. i.e., the operational procedures put in place for categories 3, 4, 5, 6 are somewhat bound to the physical limitations of the launch and re-entry phases discussed in 4.1, 4.2. Conversely categories 1, 2 (manned spacecraft, active satellites) are bound by the confines of the orbital environment discussed in 4.3. The following sections provides insight to current operational procedures to meet the risk criteria, in addition to promising Air Traffic Flow Management (ATFM) concepts and research initiatives that aim to optimise the design and handling of space operation related hazards.

5.4.1. Launch and re-entry operations

At present, the integration of space traffic into traditional airspace is being treated with a somewhat ad hoc approach. Temporary Flight Restrictions (TFR) and Special Use Airspace (SUA) are issued through Notice to Air Mans (NOTAMS), resulting in exaggerated sections of airspace segregated from traditional atmospheric traffic during launch and re-entry operations. Considering the low frequency and relatively remote locations of current spacecraft operations, the existing approach safely separates traditional air traffic from space vehicles with relatively low impact on traditional air traffic flow.

Improvements to the current segregation methods could be achieved through the implementation of the Flexible Use of Airspace (FUA) Concept during space operations [138]. Developed by EUROCONTROL in the 1990's, FUA concept moves away designating airspace as either “civil” or “military” airspace but considering it as one continuum and allocated according to user requirements. In the context of space operations this would increase the flexibility of SUA restrictions by only temporarily closing sections of airspace sectors that pose a hazard.

5.4.1.1. ATM/space operation integration concepts. Fig. 17 illustrates an excerpt of an aeronautical chart, where the exclusion zone in the airspace surrounding the US Kennedy Space Centre is represented. When considering the projected demand of future space operations [139], the static, inflexible and over conservative nature of current airspace sector closure methods severely limits future applicability. As such new strategies are being developed to appropriately size the hazard area, including Space Transition Corridors (STC) and 4 Dimensional Compact Envelopes (4DCE).

Space Transition Corridors (STC) is a concept developed by NASA to facilitate the growing demand of future space launches while simultaneously reducing the overall impact launch and re-entry operations have on the affected airspace. In contrast to the current method of space and atmospheric traffic segregation where exaggerated portions of airspace are cordoned off during launch and re-entry phases, the STC

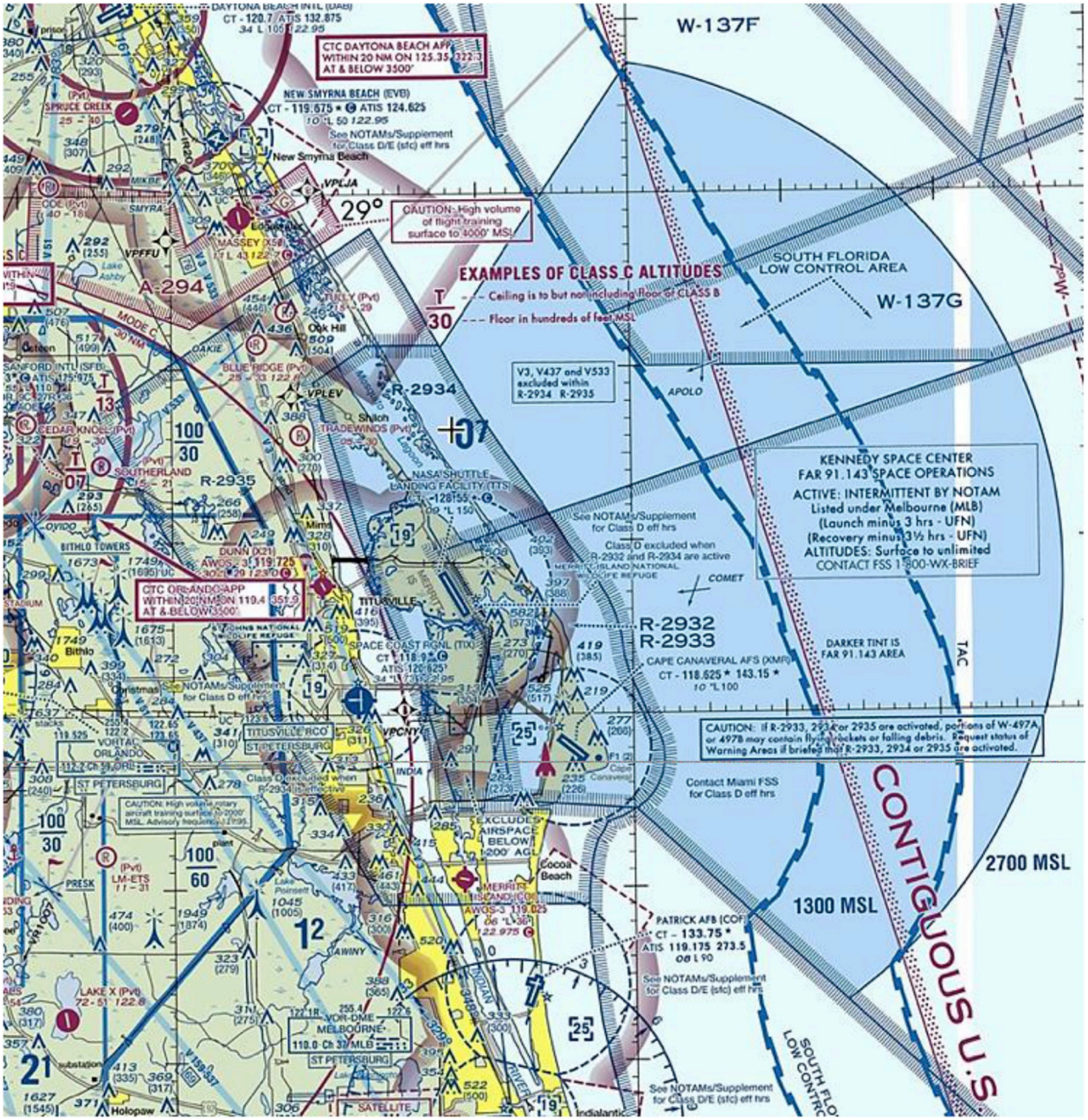

Fig. 17. Detail of aeronautical chart depicting the exclusion zone around Kennedy Space Centre during Spacecraft Launch [140].

concepts focuses on employing three spatial (length, width, azimuth) and two temporal parameters (duration and midpoint of the airspace closure time window) to create a "transition" corridor [141]. This approach has been used in sub-orbital trajectory simulations of SpaceShipTwo [142]. Unlike current airspace segregation methods, the bounds of the transition corridor are defined to equal the acceptable risk during an off-nominal event (Standard 321-07). However, similar to current segregation methods the restricted airspace (transition corridor) remains static throughout the entire flight phase, limiting its viability for next-generation spacecraft integrated air traffic operations. Proposed by Stanford University Aerospace Design Lab, 4 Dimensional Compact Envelopes are based on individual probabilistic of nominal spacecraft conditions during launch and the re-entry phases adhering to the maximum acceptable risk outlined in Standard 321-07 [36,143]. By knowing the nominal trajectory, debris catalogue, and probability of failure distribution of the spacecraft, 4D Compact Envelopes enforce only the closure of airspace that is at risk at each epoch [37]. By appropriately sizing and timing the hazard area 4D envelopes offer an elegant solution in safeguarding spacecraft operations from traditional air traffic in contrast to current airspace segregation methods. This concept is depicted in Fig. 18. Moreover, simulations using NASA's Future ATM Concepts Evaluations Tool (FACET) demonstrate that 4D Envelopes present little to no impact on traditional traffic during launch and re-entry procedures [36,37].

In practice, advanced tools that spatially and temporally optimise hazard volumes will require space vehicles to transmit accurate and timely TSPI information, requiring high performance global CNS and interoperability between all parties – an assumption that is in-line with the envisioned CNS + A enabled SWIM/TBO environment. This will also allow emerging TBO-based ATFM techniques such as *dynamic sectorisation* to become applicable. As the name implies, the dynamic sectorisation concept introduces the capability of real-time airspace

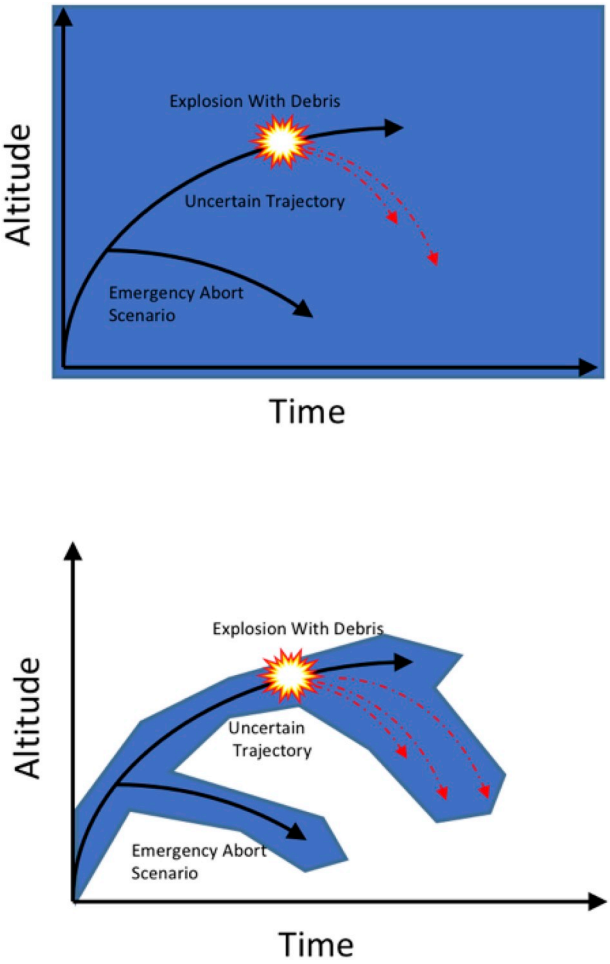

Fig. 18. 4-Dimensional Compact Envelopes (bottom) vs Current Airspace Segregation Methods (top) [37].

sector morphing with the aim of better exploiting airspace capacity and increasing efficiency while reducing operator's workload. The underlying approach is that the airspace structure adapts to future traffic flow which is inherently more predictable in the TBO environment. Based upon the current ATC sector requirement of a right prism layout, automatic two-dimensional sectorisation algorithms have demonstrated their capability of supporting real-time sector re-design, however, significant issues lies in the disruptive changes that neighbouring sectors often undergo when these methods are used. An alternative approach that aims to mitigate the unfamiliarity of operators to ATC sector changes is to introduce "Splitting and Merging" functionality, depicted in Fig. 19. Emerging research is showing, on the other hand, that an optimal control formulation based on Eulerian flow theory allows to realise a 2D plus time (2D + T) sector morphing to accommodate envisioned spatio-temporal shifts in traffic density (demand) [38]. Employing dynamic sectorisation concepts alongside advanced hazard volume tools like 4D compact envelopes has the potential to further increase spacecraft integration efficiency within the atmospheric domain [138,144].

5.4.2. On-orbit collision avoidance

Due to the non-cooperative nature of space debris, an inherently higher threat exists between a spacecraft-debris pair because collision with space objects 10 cm or larger have the potential to cause widespread damage. As a consequence novel methods have been proposed for the capture and/or removal of space debris. However due to the considerable operational and technical challenges associated with these methods, a single piece of debris is yet to be removed from orbit [145]. Until these methods reach operational maturity, performing evasive manoeuvres is the single most important technique in managing the risk associated with space object collision [40]. Formerly (as first used by the Space Shuttle orbiter), the strategy adopted to reduce the risk of on-orbit collisions was to perform a manoeuvre whenever an "intruding" object violated a $5 \times 2 \times 2$ km volume centred on the orbiter. This approach required the orbiter to expend 11–14 kg of propellant on average to avoid a potential collision, eventually making this approach over-conservative and operationally inadequate. Increasing research in the field of on-orbit deconfliction confirmed that significant operational advantages could be achieved if the uncertainty in a space objects position was considered when generating a "keep out" volume [146]. Specifically, this allowed state vector errors to be represented as an covariance ellipsoid centred on the objects nominal position [44]. This concept is has led to what is now commonly known as Space Object Collision Avoidance. Collision avoidance activities are routinely performed by spacecraft operators to characterise potential on orbit collision in either terms of the miss distance between the orbiting objects or in a statistical nature expressed as a probability of collision.

In the context of launch activities, Collision Avoidance on Launch Assessments (COLA) are performed before launch to meet operational risk criteria. Of large concern is the risk of collision between the launch vehicle (both payload and rocket body) and the International Space Station (ISS). As such conservative separation requirements have been put in place. These are detailed in Table 12, manned spaceflight category. If a COLA predicts that a launch vehicle will breach separation requirements then the launch window effectively goes into "black-out" over this period. Standard 321-07 recommends the duration of assessment be from 4–6 revolutions past initial LEO orbital insertion (6–9.5

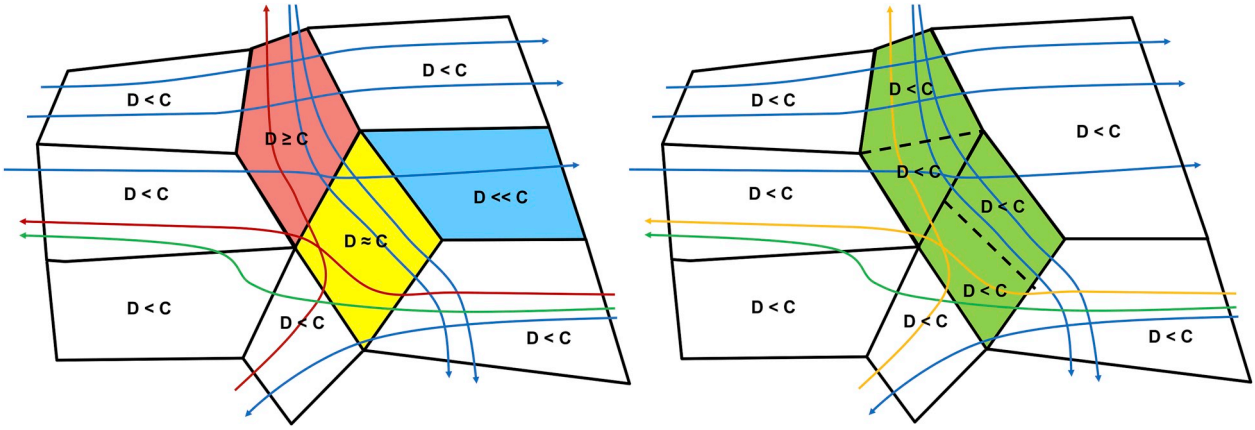

Fig. 19. Sector splitting and merging – airspace demand and capacity (D,C) before and after (left, right) sector re-design [1].

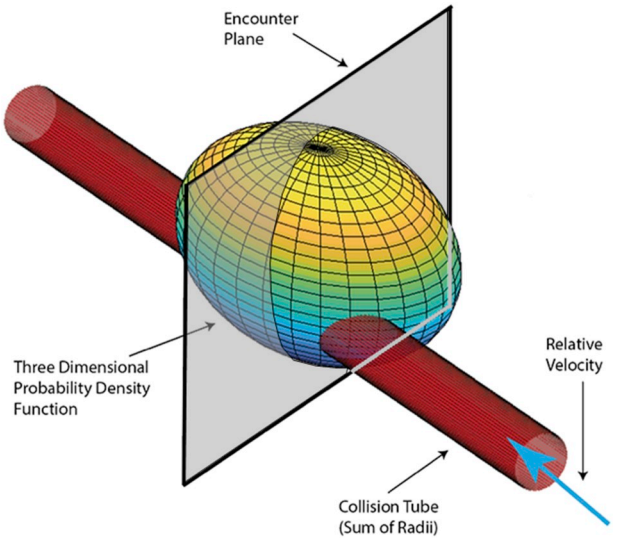

Fig. 20. 3-Dimensional encounter [148].

hours).

5.4.2.1. Modelling approach. In modelling a spacecraft collision scenario the following assumptions are typically made amongst the literature [50,147]:

1. Position uncertainty can be described by a 3D Gaussian distribution
2. The target and risk object move along straight lines at constant velocities.
3. The uncertainties in space object velocities can be neglected.
4. The target and risk object position uncertainties are Gaussian and non-correlated, therefore the covariance matrixes of both objects can be summed.
5. The position uncertainties during the encounter are constant, with corresponding covariances as at the time of closest approach.
6. The space objects size are be expressed as the sum of both radii

Fig. 20 displays the 3 dimensional collision condition, where a

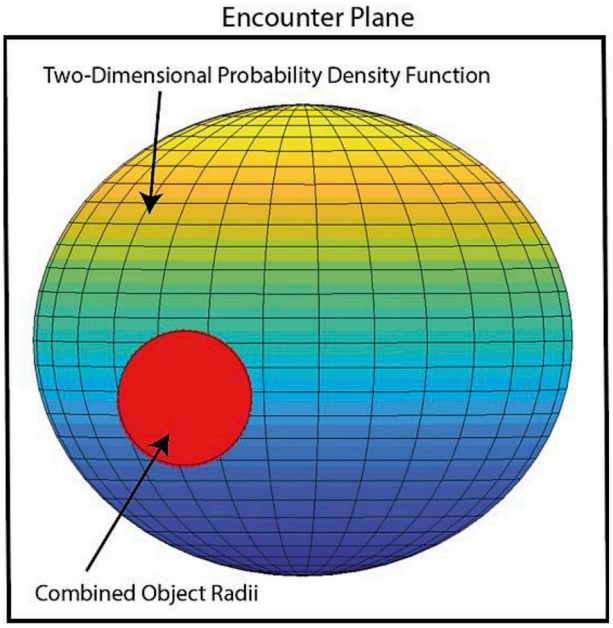

Fig. 21. 2-Dimensional encounter plane [148].

"collision tube" (of the sum of both spacecraft radii) is formed through the covariance ellipsoid. Fig. 21, on the other hand, depicts the two-dimensional encounter plane view. The magnitude of ellipsoid inflation is user-defined, but generally corresponding to an 8-sigma distribution to provide 99.999999% position assurance.

Evaluating the encounter probability can become a cumbersome task due to its high dependency on the complex dynamics of each space object and the general inability to evaluate a 3 dimensional integral any closed-form formula [50]. However, it can be shown that the probability of collision may be reduced to a two dimensional integral within the combined radii on the plane perpendicular to the relative velocity at the time of closest approach [148]. This is known as the short term encounter model. The short term encounter model is used to describe a collision scenario within the LEO environment where the typical encounter geometry of two space objects is characterized by high relative velocities and the period of encounter is in the order of seconds. Mathematically, the short term condition is expressed as the following double integral:

$$P = \frac{1}{2\,\pi\,\sigma_x\,\sigma_y} \int_{-OBJ}^{OBJ} \int_{-\sqrt{OBJ^2-x^2}}^{\sqrt{OBJ^2-x^2}} \cdot \exp\left[-\frac{1}{2}\left[\left(\frac{x-x_m}{\sigma_x}\right)^2 + \left(\frac{y-y_m}{\sigma_y}\right)^2\right]\right] dy\,dx \tag{44}$$

Where OBJ represents the combined object radii, x_m and y_m are the respective miss distance components, and $\sigma_x\,\sigma_y$ are the corresponding standard deviations.

Multiple schemes have been developed to compute the two dimensional collision probability integral, taking both numerical (Foster [45], developed for NASA ISS & Shuttle operations, Patera [44], used by Aerospace Corporation's Collision Vision Tool and Satellite Orbit Analysis Program (SOAP) [46], Alfano [47], used by Analytical Graphics STK) and analytical (Chan [48], used by Analytical Graphics STK, Garcia [50,149]) approaches. Comparative studies undertaken have provided further insight into these methods in terms of their validity, accuracy [148] and speed [150]. In any case, analytical methods demonstrate much higher performance in terms of computational speed but with decreased accuracy (however acceptable for practical purposes), where numerical methods provide the contrary. The method chosen by the user (i.e. accuracy vs time) should be driven by the specifics of the potential collision scenario in hand which extend from the planning to operational phase of spacecraft coordination [44–48,50,149].

5.4.2.2. Eliminating assumptions in collision avoidance analysis. As stated, the general approach outlined above is limited in that the assumptions made are only applicable for assessing the short-term encounter. This assumption is generally appropriate when considering LEO as the relative motion between the two space objects can be assumed linear and positional errors are zero-mean, uncorrelated, Gaussian and constant during the encounter [151]. However when considering the particular case of Geosynchronous orbits, where the relative velocity between a spacecraft pair is significantly lower than what is observed in LEO, and is now appropriately measured in the order of meters per second. The encounter region may now potentially extend up to a period of 24 hours and as a consequence the direction & magnitude of the relative velocity and combined covariance ellipsoid cannot be considered constant [48]. To account for the non-linear dynamics of the described scenario, a reformation of the overall approach is required to compute the collision probability. Alfano [151] provides a comprehensive review on the techniques that can be employed to account for non-linear encounters. Each approach follows an underlying principle of dividing the encounter into a specific finite linear regions (small discs, elongated discs, parallelepipeds) which when summed provide a total collision probability for the extended encounter.

As previously defined, the collision tube is assumed to be the

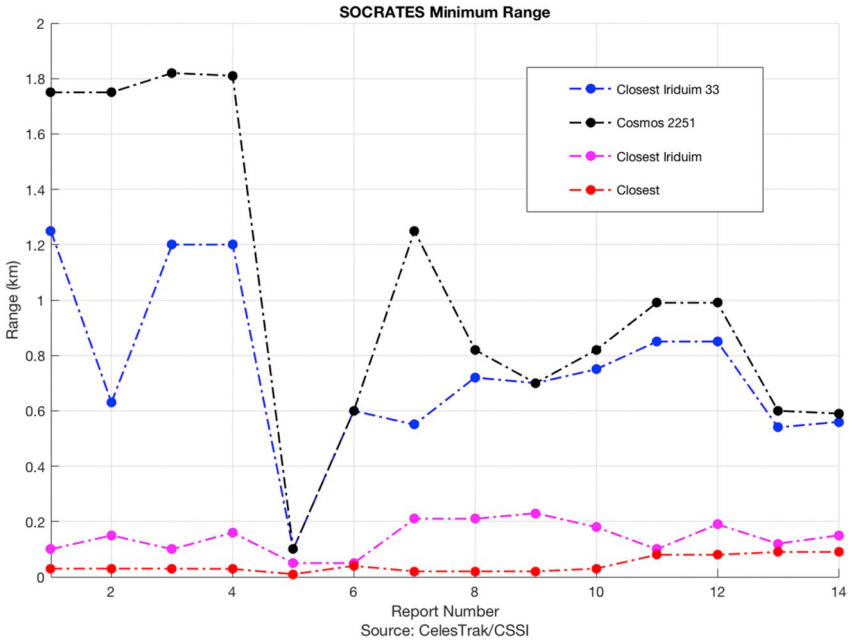

Fig. 22. Predicted close approaches of Iridium constellation and Iridium 33 with Cosmos 2251 from February 4th - 10th, 2009 [155].

combined hard-body radius of both the primary and secondary spacecraft, assuming constant altitude throughout the encounter. However, depending on the miss-distance and values of covariance of the given confliction, the need to consider the actual, 'complex' geometry of both objects may become apparent. Pulido et al. [152] demonstrates this case when covariance values are small (high orbital accuracy) compared to object size. To overcome the assumption of a combined hard-body radius, one method proposed is to calculate the Minkowski sum of the two objects [149,153].

5.4.3. On-orbit collision assessment issues

As discussed, on-orbit collision analysis is achieved through the propagation of orbital observational data where a collision warning issued if separation criteria or collision thresholds are breached. Proportional to the growth of orbital traffic, collision warnings are continually being treated as false alarms due to the high amount of uncertainty associated with current observational data [9]. The February 10th, 2009 (UTC) collision between the Iridium-33 and Cosmos 251 spacecraft, provides insight into the shortfalls of current SSA capabilities [154]. Fig. 22 displays the predicted minimum range at the time of the Iridium-Cosmos collision in terms of the closest:

- Conjunction (within the report)
- Iridium Constellation conjunctions
- Iridium 33 specific conjunctions
- Iridium 33/Cosmos 2251 conjunctions

Each of the 14 reports (2 per day) were generated by the Centre for Space Standards and Innovation (CSSI) conjunction assessment tool, SOCRATES [156] spanning from the 4th-10th February. Close approaches between Cosmos and Iridium 33 were estimated in reports 4, 5, ranging from 117 m to respectively, however, the problem therein lies that the identified conjunctions between Cosmos/Iridium 33 were consistently overshadowed by the smaller miss distances estimated in all other considered scenarios.

When interpreted by the SOCRATES ranking system (a service provided by the SOCRATES tool to identify the more probable collisions scenarios), the Iridium 33/Cosmos collision is effectively concealed from operator awareness due to greater risk of conjunctions between other objects during that period, including other Iridium spacecraft. This is displayed in Fig. 23 where the Cosmos/Iridium conjunction rank is shown in terms of the total number of collision warnings, against all other iridium related conjunction and any other Iridium-33 collision warning (within each specified report).

Nonetheless, the statistical inconsistencies observed in both Figs. 22 and 23 that effectively lead to the Iridium 33/Cosmos collision is no fault of the SOCRATES tool but due to unreliable orbital observation data. In this instance, orbital data was provided by the North American Aerospace Defence (NORAD) in the form of a Two Line Element Set (TLEs). TLEs are a specific data format used regularly by satellite operators to assess potential collision scenarios and conduct orbital manoeuvres if required. TLEs contain the following object related information at a given epoch:

- Line Number
- Classification
- Epoch
- Drag Term
- Checksum
- Right Ascension of the ascending node
- Mean Motion
- Satellite Number
- International Designator
- Mean Motion Derivative(s)
- Element Set number
- Inclination
- Argument of Perigee
- Revolution Number

TLEs data structure is specific to the use of simplified perturbation models SGP4, SDP4, where the former is tailored for near space object propagation (orbital period of less than 225 min) and the latter for deep space (orbital period greater than or equal to 225 min). Detailed information of the algorithms employed in special perturbation models can be found in Ref. [157]. TLEs are generated from measurements made by the US Space Surveillance Network (SSN), a global network of predominantly ground based optical and radar (mechanical and phased array) sensors. The SSN plays a critical role in tracking and cataloguing non-cooperative RSO, however, the required accuracy for credible collision detection cannot be reached through the use of TLEs and associated propagators exclusively [155,158,159].

Despite well documented shortfalls, the advantage of providing a compact, easily attainable form of RSO information has led to TLEs widespread use among the satellite industry. As such there has been continued research efforts to improve the fidelity of TLEs and related applications [160]. Nonetheless, a lack of meaningful covariance and planned manoeuvre information introduces significant uncertainty

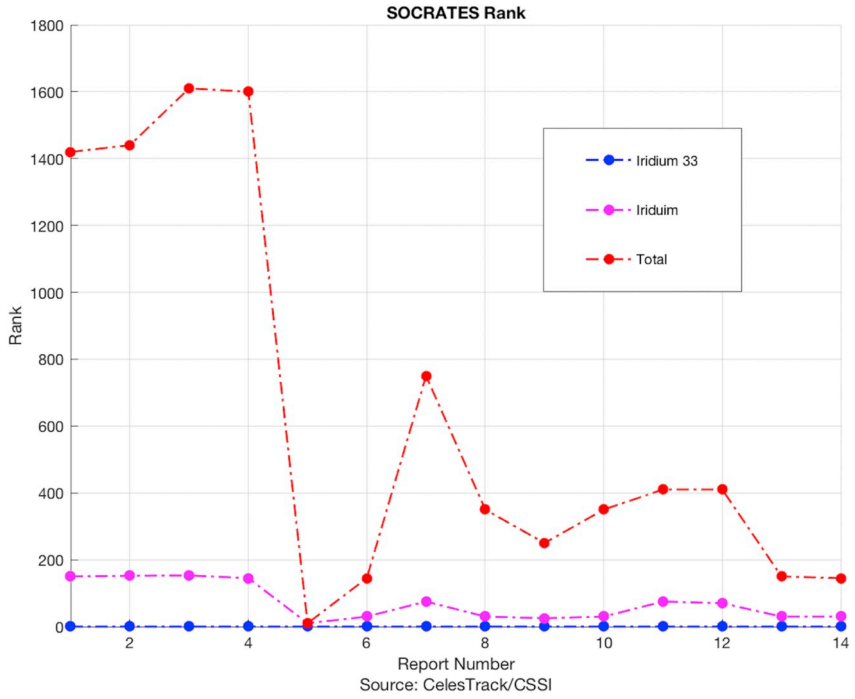

Fig. 23. Ranking of predicted close approaches of Iridium, Iridium 33 and Cosmos 2251 from February 4th - 10th, 2009 [155].

(particularly for long term predictions), and as such it is best practice amongst satellite operators to treat assessments purely based on TLEs as a coarse indication of collision risk initiating what is known as the “two tier” model. To overcome the shortfalls of TLEs data, the satellite operator will then commonly use the precise owner operator ephemeris data, and in the case of non-cooperative collision scenario, special perturbation (SP) information of the “intruding object” can be requested when possible from the Joint Space Operations Centre (JSpOC). As a result of more precise orbital data the additional screening will then reduce the severity of the collision risk and if necessary, more pertinent manoeuvre(s) can be performed [161].

In exchange for more authoritative data comes with it the additional delays associated with the manual collection process and conceivably the reduced effectiveness of any actionable protocol that may be required. Because of this, the risk associated with a two tier process are still seen as overall insufficient and an infective way to perform collision screening [158]. In the interest of improved SSA capabilities, significant progress has been made for more effective data sharing methods amongst satellite community. SOCRATES-GEO, an automated conjunction analysis process offered by the Centre for Space Standards and Innovation (CSSI), generates conjunction analysis through the use of owner operator-supplied ephemeris data. Originally developed in mind of GEO operations, SOCRATES-GEO has now extended to LEO environment with a total of 286 operational satellites (as of 2010) sharing precise ephemeris data [162].

A user-centric approach to data collection reduces the frequency of a two-tier model as user cooperative conjunctions scenarios can be managed with a single forecast. Clearly, sharing precise satellite ephemeris data is under discretion of the owner-operator, as in some circumstances disclosing planning manoeuvre information may compromise the mission of the spacecraft. Nonetheless, it is important that complete ephemeris data should be shared whenever possible due to the implications that almost certain intermediate manoeuvres have on collision assessment validity [162]. In any case, there is general consensus that a sensor- and mission-centric information sharing scheme akin to the current services provided by CSSI will be essential aspect of an STM system.

Of utmost importance will be the *transparency* and *traceability* of all available data - An increase alone will not solve the current issue of RSO ambiguity and collision avoidance subjectivity, confidence building measurements must also be readily available to all operators. This would include (but not limited to); the amount, type and performance of the sensor(s), adopted coordinate systems and time (including clock accuracy), and where possible physical states and parameters, functional characteristics and mission objectives. To effectively distribute this information and support the use of big data analytics, the adoption of standardised RSO ontologies was proposed [163,164]. Further, through the use of high definition photometry and the principles of biometrics, novel methods are being developed that aim to uniquely characterise RSO in the form of "fingerprints" and progress towards a Unique RSO (URSO) database [166,167]. Through realisation of the above elements, the traditional SSA approach can be elevated to “Encompass all elements in the space environment as well as operators and human decision makers and ground-based elements that affect space activities” [9]. Which, in practical terms will allow “The actionable knowledge required to predict, avoid, deter, operate through, recover from, and/or attribute cause to the loss and/or degradation of space capabilities and services” [9]. This vision encapsulates a concept that is referred to as Space Domain Awareness (SDA). In essence, an SDA approach to a future STM system will enable intelligent decision-making tools to ensure timely, reliable threat and hazard identification and prediction within the orbital domain [9,154,165] while also harmonising the interfaces between the atmospheric and near space environment in the context of future space transport operations.

6. Conclusions

Significant efforts are being made to develop novel spacecraft platforms that re-define how space and atmospheric flight phases are accomplished. Within the atmospheric domain new-entrants performing point-to-point operations will require a global multi spaceport network in proximity of major metropolitan hubs. As such, the continued use of current segregation type methods is not a viable option and would be extremely detrimental to the global aviation industry, emphasising the necessity for new-entrant spacecraft to transition to mixed flow Trajectory Based Operations (TBO). In enabling this, novel

operational concepts such as Space Transition Corridors (STC) and Four Dimensional Compact Envelopes (4DCE) have been proposed. These concepts make use of precise Time and Space Position Information (TSPI) provided by advanced Communication, Navigation and Surveillance/Air Traffic Management and Avionics (CNS + A) technology to optimise hazard volumes and increase airspace efficiency and capacity. Nevertheless, the proposed concepts are still very much in their infancy, calling for continued research efforts that focus on Air Traffic Management/Space Traffic Management (ATM/STM) harmonisation and novel spacecraft-focused Air Traffic Flow Management (ATFM) techniques. The introduction of these technologies should fundamentally base upon new-entrant platform performance, and the physical and computational limitations identified in both re-entry and launch trajectory planning methodologies. Additionally, the environmental sustainability of atmospheric operations needs to be further verified as pertinent subjects such as spacecraft gaseous emissions and noise are not well documented in the literature.

Regarding the on-orbit phase, the unique hazards associated with space weather events represent an important problem to be addressed. However, the main challenges poised to future STM will be the avoidance/mitigation of on-orbit collisions. Post mission disposal manoeuvres with the aim to mitigate space debris generation within the Low-Earth Orbit (LEO) and Geostationary Orbit (GEO) regions are currently under various levels of ISO standardisation. Studies demonstrate that the effectiveness of these strategies is fundamentally dependent on operational compliance levels, where an increase in current disposal efforts is required to preserve operational sustainability.

Continued research in the areas of stochastic spaceflight mechanics within the on-orbit environment has seen the development of sound collision broadcast methodologies that are widely used in industry. However, a growing number of false alarms due to unreliable observational data highlights the need for a future STM system to adopt cyber-physical architectures based on advanced networking, computing and control technologies to ensure space object data fidelity and to increase the reliability of predictions. Current standards and guidelines form an initial basis for the definition of a viable STM infrastructure however, continued efforts are required to delineate a code of conduct, and an equivalent rules of the “air” to define operation norms and enforce standards for space transport operations. Moreover, a lack of certification standards of CNS + A systems above FL600 demands inquest into the actual performance of these systems within and above the near space region as only then can cyber-physical system architectures be confidently developed and deployed on a global scale to support a fully integrated (i.e., compatible and interoperable) ATM/STM network.

References

[1] M. Sippel, Introducing the SpaceLiner Vision, (2007).
[2] M. Vozoff, J. Couluris, SpaceX products-advancing the use of space, AIAA SPACE 2008 Conference \& Exposition, vol. 9, 2008.
[3] R.D. Howard, et al., Dream chaser commercial crewed spacecraft overview, 17th AIAA International Space Planes and Hypersonic Systems and Technologies Conference, 2011.
[4] D. Linehan, Spaceshipone: an Illustrated History, Zenith Press, 2011.
[5] R. Longstaff, A. Bond, The SKYLON project, 17th AIAA International Space Planes and Hypersonic Systems and Technologies Conference, 2011.
[6] R.A.M. Hunter, Point-to-point Commercial Space Transportation in National Aviation System, (2010).
[7] P. Duan, ADS-B feasibility study for commercial space flight operations, Digital Avionics Systems Conference (DASC), IEEE/AIAA, 201029th, 2010, pp. 3-A.
[8] R. VanSuetendael, A. Hayes, R. Birr, A common communications, navigation & surveillance infrastructure for accommodating space vehicles in the next generation air transportation system, AIAA 2008-6893, AIAA Atmospheric Flight Mechanics Conference and Exhibit, 2008.
[9] M.J. Holzinger, M.K. Jah (Eds.), Challenges and Potential in Space Domain Awareness, 2018.
[10] T. Flohrer, H. Krag, H. Klinkrad, T. Schildknecht, Feasibility of performing space surveillance tasks with a proposed space-based optical architecture, Adv. Space Res. 47 (6) (2011) 1029–1042.
[11] J. Utzmann and A. Wagner, "SBSS Demonstrator: a Space-based Telescope for Space Surveillance and Tracking," ed.
[12] Y.-W. Chang, The first decade of commercial space tourism, Acta Astronaut. 108 (2015) 79–91.
[13] D.J. Piatak, M.K. Sekula, R.D. Rausch, Ares launch vehicle transonic buffet testing and analysis techniques, J. Spacecraft Rockets 49 (5) (2012) 798–807.
[14] J.P.W. Stark, The spacecraft environment and its effect on design, in: P.W. Fortescue, G.G. Swinerd, J.P.W. Stark (Eds.), Spacecraft Systems Engineering, fourth ed., Wiley, 2011.
[15] Z. Shen, P. Lu, Onboard generation of three-dimensional constrained entry trajectories, J. Guid. Contr. Dynam. 26 (1) (2003) 111–121.
[16] Z. Shen, P. Lu, On-board entry trajectory planning for sub-orbital flight, Acta Astronaut. 56 (6) (2005) 573–591.
[17] P. Lu, P. Rao, An integrated approach for entry mission design and flight simulations, *42nd* AIAA Aerospace Sciences Meeting and Exhibit, 2004, p. 702.
[18] P. Lu, Entry guidance and trajectory control for reusable launch vehicle, J. Guid. Contr. Dynam. 20 (1) (1997) 143–149.
[19] P. Lu, Asymptotic analysis of quasi-equilibrium glide in lifting entry flight, J. Guid. Contr. Dynam. 29 (3) (2006) 662–670.
[20] K.D. Mease, D.T. Chen, P. Teufel, H. Sch-ograve, nenberger, Reduced-order entry trajectory planning for acceleration guidance, J. Guid. Contr. Dynam. 25 (2) (2002) 257–266.
[21] A. Saraf, J.A. Leavitt, D.T. Chen, K.D. Mease, Design and evaluation of an acceleration guidance algorithm for entry, J. Spacecraft Rockets 41 (6) (2004) 986–996.
[22] K.-U. Schrogl, Space traffic management: the new comprehensive approach for regulating the use of outer space — results from the 2006 IAA cosmic study, Space Pol. 62 (2008) 272–276.
[23] C. Contant-Jorgenson, P. Lala, and K.-U. Schrogl, The international academy of astronautics (IAA) cosmic study on space traffic management, Presented at the United Nations Committee on the Peaceful Uses of Outer Space (UNCOPUOS). ([Online]. Available:).
[24] H. Cukurtepe, I. Akgun, Towards space traffic management system, Acta Astronaut. 65 (2009) 870–878.
[25] W.K. Tobiska, The space environment, in: J.R. Wertz, D.F. Everett, J.J. Puschell (Eds.), Space Mission Engineering: the New SMAD, Microcosm Press, 2011.
[26] B. Arbesser-Rastburg, N. Jakowski, Effects on satellite navigation, in: V. Bothmer, I. Daglis (Eds.), Space Weather - Physics and Effects, Springer-Verlag Berlin Heidelberg, 2007, pp. 353–382.
[27] J.-G. Wu, L. Eliasson, H. Lundstedt, A. Hilgers, L. Andersson, O. Norberg, Space environment effects on geostationary spacecraft: analysis and prediction, Adv. Space Res. 26 (1) (2000) 31–36.
[28] N. Iucci, et al., Space weather conditions and spacecraft anomalies in different orbits, Space Weather 3 (1) (2005) 1–16.
[29] Y.-z. Luo, Z. Yang, A review of uncertainty propagation in orbital mechanics, Prog. Aero. Sci. 89 (2017) 23–39.
[30] S. Ramasamy, R. Sabatini, and A. Gardi, "A unified analytical framework for aircraft separation assurance and UAS sense-and-avoid," Journal of Intelligent \& Robotic Systems, pp. 1-20.
[31] I.-A.S.D.C. Committee, IADC-02-01 Revision, IADC Space Debris Mitigation Guidelines vol. 1, (2007).
[32] A. Kato, B. Lazare, D. Oltrogge, P. Stokes, Standardization by ISO to ensure the sustainability of space activities, Proceedings of the Sixth European Conference on Space Debris, ESOC, Darmstadt, Germany, 2013, pp. 22–25.
[33] S. Winkler, et al., GPS Receiver On-orbit Performance for the GOES-R Spacecraft, (2017).
[34] B. Hudson, AN/MPS-39 support of US space launch activities, Radar Conference, 1995, Record of the IEEE 1995 International, 1995, pp. 39–43.
[35] Terminal guidance system for satellite rendezvous," Journal of the Aerospace Sciences, vol. 27, no. 9, pp. 653-658, 1960/09/01 1960.
[36] J.E. Young, M.G.E. Kee, C.M. Young, Effects of future launch and reentry operations on the national airspace system, J. Air Transp. 25 (1) (2017) 8–16.
[37] T.J. Colvin, J.J. Alonso, Compact envelopes and SU-FARM for integrated air-and-space traffic management, AIAA Aerospace Sciences Meeting, 2015.
[38] T. Kistan, A. Gardi, R. Sabatini, S. Ramasamy, E. Batuwangala, An evolutionary outlook of air traffic flow management techniques, Progress in Aerospace Sciences 88 (2017) 15–42.
[39] D.J. Kessler, N.L. Johnson, J.C. Liou, M. Matney, The kessler syndrome: implications to future space operations, Advances in the Astronautical Sciences 137 (8) (2010).
[40] D.J. Kessler, Orbital debris environment for spacecraft in low earth orbit, Journal of spacecraft and rockets 28 (3) (1991) 347–351.
[41] N.L. Johnson, A new look at the GEO and near-GEO regimes: operations, disposals, and debris, Acta Astronautica 80 (2012) 82–88.
[42] H. Krag, S. Lemmens, T. Flohrer, H. Klinkrad, Global trends in achieving successful end-of-life disposal in LEO and GEO, SpaceOps 2014 Conference, 2014, p. 1933.
[43] J.-C. Liou, P. Krisko, An Update on the Effectiveness of Postmission Disposal in LEO, (2013).
[44] R.P. Patera, General method for calculating satellite collision probability, Journal of Guidance, Control, and Dynamics 24 (4) (2001) 716–722.
[45] J.L. Foster, H.S. Estes, A parametric analysis of orbital debris collision probability and maneuver rate for space vehicles, NASA JSC 25898 (1992).
[46] R.P. Patera, G.E. Peterson, Space vehicle maneuver method to lower collision risk to an acceptable level, Journal of guidance, control, and dynamics 26 (2) (2003) 233–237.
[47] S. Alfano, A numerical implementation of spherical object collision probability, Journal of Astronautical Sciences 53 (1) (2005) 103–109.

[48] F.K. Chan, Spacecraft Collision Probability, Aerospace Press El Segundo, CA, 2008.
[49] R. Garcia-Pelayo, J. Hernando-Ayuso, Series for collision probability in short-encounter model, Journal of Guidance, Control, and Dynamics (2016) 1908–1916.
[50] R. Serra, D. Arzelier, M. Joldes, J.-B. Lasserre, A. Rondepierre, B. Salvy, Fast and accurate computation of orbital collision probability for short-term encounters, Journal of Guidance, Control, and Dynamics (2016) 1009–1021.
[51] A. Gardi, R. Sabatini, S. Ramasamy, Multi-objective optimisation of aircraft flight trajectories in the ATM and avionics context, Progress in Aerospace Sciences 83 (2016) 1–36.
[52] N. P. Y.Lim, A. Gardi and R.Sabatini, Eulerian optimal control formulation for dynamic morphing of airspace sectors, Presented at the 31st Congress of the International Council of the Aeronautical Sciences. ([Online]. Available:).
[53] P. H. Kopardekar, Safely enabling UAS operations in low-altitude airspace, Presented at the NASA UAS Traffic Management (UTM). ([Online]. Available:).
[54] NASA, UTM: Air Traffic Management for Low-altitude Drones, N. A. a. S. A. (NASA), Washington DC, USA, 2015 NASAfacts NF-2015-10-596-HQ.
[55] J. Homola, T. Prevot, J. Mercer, N. Bienert, C. Gabriel, UAS traffic management (UTM) simulation capabilities and laboratory environment, 35th DASC Digital Avionics Systems Conference, DASC 2016, 2016 2016-(December).
[56] P. Kopardekar, J. Rios, T. Prevot, M. Johnson, J. Jung, J.E. Robinson III, Unmanned aircraft system traffic management (UTM) concept of operations, 16th AIAA Aviation Technology, Integration, and Operations Conference, 2016.
[57] T. Prevot, J. Homola, J. Mercer, From rural to urban environments: human/systems simulation research for low altitude UAS traffic management (UTM), 16th AIAA Aviation Technology, Integration, and Operations Conference, 2016.
[58] E. Mueller, P. Kopardekar, K. Goodrich, Enabling airspace integration for high-density on-demand mobility operations, 17th AIAA Aviation Technology, Integration, and Operations Conference, 2017.
[59] S. Ramasamy, R. Sabatini, A. Gardi, J. Liu, LIDAR obstacle warning and avoidance system for unmanned aerial vehicle sense-and-avoid, Aerosp Sci Technol 55 (2016) 344–358.
[60] S. Ramasamy, R. Sabatini, A. Gardi, A unified analytical framework for aircraft separation assurance and UAS sense-and-avoid, J Intell Rob Syst Theor Appl 91 (3–4) (2018) 735–754.
[61] S. Ramasamy, R. Sabatini, A. Gardi, A novel approach to cooperative and non-cooperative RPAS detect-and-avoid, SAE Techni. Paper, 2015 vol. 2015-September, no. September.
[62] E. Batuwangala, T. Kistan, A. Gardi, R. Sabatini, Certification challenges for next-generation avionics and air traffic management systems, IEEE Aerosp Electron Syst Mag 33 (9) (2018) 44–53.
[63] S. Ramasamy, R. Sabatini, A. Gardi, Avionics sensor fusion for small size unmanned aircraft Sense-and-Avoid, 2014 IEEE International Workshop on Metrology for Aerospace, MetroAeroSpace, Benevento, 2014, pp. 271–276.
[64] S. Ramasamy, A. Gardi, J. Liu, R. Sabatini, A laser obstacle detection and avoidance system for manned and unmanned aircraft applications, Int. Conf. Unmanned Aircr. Syst, ICUAS, 2015, pp. 526–533.
[65] R. Sabatini, T. Moore, S. Ramasamy, Global navigation satellite systems performance analysis and augmentation strategies in aviation, Progress in Aerospace Sciences 95 (2017) 45–98.
[66] R. Sabatini, T. Moore, C. Hill, A new avionics-based GNSS integrity augmentation system: Part 1 - Fundamentals, J. Navig. 66 (3) (2013) 363–384.
[67] R. Sabatini, T. Moore, C. Hill, S. Ramasamy, Investigation of GNSS integrity augmentation synergies with unmanned aircraft sense-and-avoid systems, SAE Techni. Paper, 2015 vol. 2015-September, no. September.
[68] L. Felicetti, M.R. Emami, A multi-spacecraft formation approach to space debris surveillance, Acta Astronautica 127 (2016) 491–504.
[69] X. Vanwijck, T. Flohrer, Possible Contribution of Space-based Assets for Space Situational Awareness vol. 4, (01 2008), pp. 2466–2472.
[70] M. Gruntman, Passive optical detection of submillimeter and millimeter size space debris in low Earth orbit, Acta Astronautica 105 (1) (2014) 156–170.
[71] J. Utzmann, et al., Space-based Space Surveillance and Tracking Demonstrator: Mission and System Design, (2014).
[72] J.G. Reed, et al., Performance efficient launch vehicle recovery and reuse, Presented at the AIAA SPACE, 2016 ([Online]. Available:).
[73] D.E. Koelle, R. Janovsky, Development and transportation costs of space launch systems, Presented at the DGLR/CEAS European Air and Space Conference, 2007 ([Online]. Available:).
[74] L.A. Davis, First stage recovery, Engineering 2 (2016) 152–153.
[75] T.A. Heppenheimer, The Space Shuttle Decision: NASA's Search for a Reusable Space Vehicle, (1999) NASA/SP-1999-4221.
[76] E. Seedhouse, Virgin Galactic: the First Ten Years, Springer International Publishing, 2015.
[77] M. Hempsell, A. Bond, Skylon: an example of commercial launcher system development, Journal of the British Interplanetary Society 67 (2014) 434–439.
[78] S. Lentz, M. Hornung, W. Staudacher, Conceptual design of winged reusable two-stage-to-orbit space transport systems, Basic Research and Technologies for Two-stage-to-orbit Vehicles, Wiley, 2006.
[79] S. Paul, T. Westbrook, Tesla chief Musk's latest idea: intercity rocket travel, [Online]. Available: https://www.reuters.com/article/us-space-mars/tesla-chief-musks-latest-idea-intercity-rocket-travel-idUSKCN1C40MF, (Sep 2017) , Accessed date: 3 July 2018.
[80] T. Masson-Zwaan, S. Freeland, Between heaven and earth: the legal challenges of human space travel, Acta Astronautica 66 (2010) 1597–1607.
[81] A. Tewari, Atmospheric and Space Flight Dynamics, Springer, 2007.
[82] T. Wekerle, J.B.P. Fiho, L.E.V.L. da Costa, L.G. Trabasso, Status and trends of smallsats and their launch vehicles - an up-to-date review, Journal of Aerospace Technology Management 7 (3) (2017) 269–286.
[83] C. Niederstrasser and W. Frick, Small launch vehicles - a 2016 state of the industry survey, Presented at the 67th International Astronautical Congress. ([Online]. Available:).
[84] M. Sippel, J. Klevanski, A. van Foreest, l. G\"u Ali, B. Esser, M. Kuhn, The SpaceLiner Concept and its Aerothermodynamic Challenges, (2006).
[85] F.G. von der Dunk, The integrated approach — regulating private human space-flight as space activity, aircraft operation, and high-risk adventure tourism, Acta Astronautica 92 (2013) 199–208.
[86] P.E. Davies, *North American X-15,* (X-planes), Osprey Publishing, 2017.
[87] K. J. Stroud and S. E. Jacobs, Dream chaser integrated spacecraft and pressure suit design, Presented at the 45th International Conference on Environmental Systems. ([Online]. Available:).
[88] R. Varvill, A. Bond, A comparison of propulsion concepts for SSTO reusable launchers, Journal of the British Interplanetary Society 56 (2003) 108–117.
[89] K. Gee and S. L. Lawrence, Launch vehicle debris models and crew vehicle ascent abort risk, Presented at the 2013 Proceedings Annual Reliability and Maintainability Symposium (RAMS). ([Online]. Available:).
[90] R. Daines, C. Segal, Combined rocket and airbreathing propulsion systems for space-launch applications, J Propul Power 14 (5) (1998) 605–612.
[91] S. Walker, M. Tang, and C. Mamplata, TBCC propulsion for a Mach 6 hypersonic airplane, Presented at the 16th AIAA/DLR/DGLR International Space Planes and Hypersonic Systems and Technologies Conference. ([Online]. Available:).
[92] U. Hueter, Rocket-based combined-cycle propulsion technology for access-to-space applications, Presented at the 9th International Space Planes and Hypersonic Systems and Technologies. ([Online]. Available:).
[93] G. Norris, Skunk Works Hints at SR-72 Demonstrator Progress, (Jun 2017) [Online]. Available: http://aviationweek.com/defense/skunk-works-hints-sr-72-demonstrator-progress , Accessed date: 3 July 2018.
[94] G. Hagemann, H. Immich, T.V. Nguyen, G.E. Dumnov, Advanced rocket nozzles, J Propul Power 14 (5) (1998) 620–634.
[95] W. Huang, Z.-G. Wang, D.B. Ingham, L. Ma, M. Pourkashanian, Design exploration for a single expansion ramp nozzle (SERN) using data mining, Acta Astronautica 83 (2013) 10–17.
[96] Z. Liang, J. Yu, Z. Ren, Q. Li, Trajectory planning for cooperative flight of two hypersonic entry vehicles, 21st AIAA International Space Planes and Hypersonics Technologies Conference, 2017, p. 2251.
[97] N.X. Vinh, A. Busemann, R.D. Culp, Hypersonic and planetary entry flight mechanics, NASA STI/Recon Technical Report A 81 (1980).
[98] C. D. Johnson and P. S. Wilke, Protecting satellites from the dynamics of the launch environment, Presented at the AIAA Space 2003 Conference & Exposition. ([Online]. Available:).
[99] D.M. Van Wie, D.G. Drewry Jr., D.E. King, C.M. Hudson, The hypersonic environment: required operating conditions and design challenges, Journal of Materials Science 39 (19) (2004) 5915–5924.
[100] J.C. Harpold, C.A. Graves Jr., Shuttle entry guidance, American Astronautical Society, Anniversary Conference, 25th, Houston, Tex., Oct. 30-Nov. 2, 1978, vol. 1, 1978, p. 35.
[101] J.C. Harpold, D.E. Gavert, Space shuttle entry guidance performance results, Journal of Guidance, Control, and Dynamics 6 (6) (1983) 442–447.
[102] F.J. Regan, Dynamics of Atmospheric Re-entry, Aiaa, 1993.
[103] Y. Xie, L. Liu, J. Liu, G. Tang, W. Zheng, Rapid generation of entry trajectories with waypoint and no-fly zone constraints, Acta Astronautica 77 (2012) 167–181.
[104] W.L. Pritchard, J.A. Sciulli, Satellite Communication Systems Engineering, Prentice Hall Englewood Cliffs, New Jersey, 1993.
[105] A. Dalgarno, R.J.W. Henry, A.L. Stewart, The photoionization of atomic oxygen, Planetary and Space Science 12 (3) (1964) 235–246.
[106] E. Doornbos, H. Klinkrad, Modelling of space weather effects on satellite drag, Advances in Space Research 37 (6) (2006) 1229–1239.
[107] R.L. Walterscheid, Solar cycle effects on the upper atmosphere - implications for satellite drag, Journal of Spacecraft and Rockets 26 (1989) 439–444.
[108] D.M. Prieto, B.P. Graziano, P.C.E. Roberts, Spacecraft drag modelling, Progress in Aerospace Sciences 64 (2014) 56–65.
[109] A. Hilgers, A. Glover, E. Daly, Effects on spacecraft hardware and operation, in: V. Bothmer, I. Daglis (Eds.), Space Weather - Physics and Effects, Springer-Verlag Berlin Heidelberg, 2007, pp. 353–382.
[110] A.K. Singh, D.S. Siingh, R.P. Singh, Space weather: physics, effects and predictability, Surveys in Geophysics 31 (6) (2010) 581–638.
[111] L.J. Lanzerotti, Space weather effects on communications, in: V. Bothmer, I. Daglis (Eds.), Space Weather - Physics and Effects, Springer-Verlag Berlin Heidelberg, 2007, pp. 247–268.
[112] K.K. de Groh, B.A. Banks, C.E. McCarthy, R.N. Rucker, L.M. Roberts, L.A. Berger, MISSE PEACE Polymers Atomic Oxygen Erosion Results, (2006) NASA/TM-2006-214482.
[113] W.A.D. Greer, J.P.W. Stark, N.H. Pratt, Surface-induced luminescence in a high-velocity rarefied atomic oxygen flow regime, Journal of Geophysical Research - Space Physics 100 (A5) (1995) 7821–7828.
[114] E. Grossman, I. Gouzman, Space environment effects on polymers in low earth orbit, Nuclear Instruments and Methods in Physics Research Section B: Beam Interactions with Materials and Atoms 208 (2003) 48–57.
[115] J.-C. Liou, N.L. Johnson, Risks in space from orbiting debris, Science 311 (5759) (2006) 340–341.
[116] M. Stanford, J.A. Jones, Space radiation concerns for manned exploration, Acta Astronautica 45 (1) (1999) 39–47.
[117] R. Facius, G. Reitz, Space weather impacts on space radiation protection, in: V. Bothmer, I. Daglis (Eds.), Space Weather - Physics and Effects, Springer-Verlag

Berlin Heidelberg, 2007, pp. 289–352.
[118] RTCA DO-340: Concept of Use (CONUSE) for Aeronautical Information Services (AIS) and Meteorological (MET) Data Link Services, RTCA DO-340, (2012).
[119] RTCA DO-324: Safety and Performance Requirements (SPR) for Aeronautical Information Services (AIS) and Meteorological (MET) Data Link Services, RTCA DO-324, (2010).
[120] RTCA DO-308: Operational Services and Environment Definition (OSED) for Aeronautical Information Services (AIS) and Meteorological (MET) Data Link Services, RTCA DO-308, (2007).
[121] ICAO, Annex 3 to the Convention on International Civil Aviation - Meteorological Service for International Air Navigation," I. C. A. O. (ICAO), Montreal, Canada, (2010).
[122] A. Gardi, Y. Lim, T. Kistan, R. Sabatini, Planning and negotiation of optimized 4D-trajectories in strategic and tactical rerouting operations, 30th Congress of the International Council of the Aeronautical Sciences, ICAS 2016, 2016.
[123] E. Canuto, C. Novara, L. Massotti, D. Carlucci, C.P. Montenegro, Chapter 8 - orbit and attitude sensors, Spacecraft Dynamics and Control, Butterworth-Heinemann, 2018, pp. 389–461.
[124] M.D. Griffin, Space Vehicle Design, AIAA, 2004.
[125] Y. Sun, M. Kumar, Uncertainty propagation in orbital mechanics via tensor decomposition, Celestial Mechanics and Dynamical Astronomy 124 (3) (2016) 269–294.
[126] A. Gelb, Applied Optimal Estimation, MIT press, 1974.
[127] A. Gelb, R.S. Warren, Direct statistical analysis of nonlinear systems: CADET, AIAA Journal 11 (5) (1973) 689–694.
[128] T.C.O. Brown, M. Gleason, M. Hallax, A. Long, E. Rivera, D. Finkleman, T. Hitchens, M. Jah, D. Koplow, R. Sedwick, Orbital Traffic Management Study: Final Report, (2016).
[129] P.B. Larsen, Space traffic management standards, Journal of Air Law and Commerce 83 (2) (2018) 359.
[130] I.-A.S.D.C. Committee, Support to the IADC Space Debris Mitigation Guidelines vol. 1, (2014) IADC-04-06 Rev 5.5.
[131] N.L. Johnson, Medium Earth Orbits: Is There a Need for a Third Protected Region? (2010).
[132] D.S. McKnight, F.R. Di Pentino, New insights on the orbital debris collision hazard at GEO, Acta Astronautica 85 (2013) 73–82.
[133] R.S. Jakhu, Regulatory Process for Communications Satellite Frequency Allocations," Handbook of Satellite Applications, (2017), pp. 359–381.
[134] Y. Henri, Orbit/spectrum INternational regulatory framework: challenges in the 21st century, Presented at the 6th Nandasiri Jasentuliyana Keynote Lecture. ([Online]. Available:).
[135] J. Hoffman and J. N. Pelton, "Regulatory Procedures and Standards for Launch Range Safety for Manned and Unmanned Launches-(Chapter 9)".
[136] A.G. Karacalioglu, A. Bukley, Examining the underlying causes of space launch failures, Space Safety Is No Accident, Springer, 2015, pp. 179–188.
[137] P.D. Wilde, C. Draper, Aircraft protection standards and implementation guidelines for range safety, Proc. 48 *th* AIAA Aerospace Sciences Meeting, vol. 1542, Paper AIAA, 2010.
[138] S. Kaltenhaeuser, F. Morlang, D.-R. Schmitt, A Concept for Improved Integration of Space Vehicle Operation into ATM, (2017).
[139] E. Seedhouse, Suborbital: Industry at the Edge of Space, Springer Science \& Business Media, 2014.
[140] SkyVector: Flight Planning/Aeronautical Charts, Available: https://skyvector.com.
[141] K.D. Bilimoria, M. Jastrzebski, Space transition corridors in the national airspace system, Aviation Technology, Integration, and Operations Conference, Los Angeles, CA, 2013.
[142] P. Llanos, E. Seedhouse, C. Hays, Nominal SpaceShipTwo Flights Conducted by Scientist-astronaut Candidates in a Suborbital Space Flight Simulator, (2018).
[143] T.J. Colvin, J.J. Alonso, Near-elimination of airspace disruption from commercial space traffic using compact envelopes, AIAA SPACE 2015 Conference and Exposition, 2015, p. 4492.
[144] T. Standfuß, I. Gerdes, A. Temme, M. Schultz, Dynamic airspace optimisation, CEAS Aeronautical Journal 9 (3) (2018) 517–531.
[145] M. Shan, J. Guo, E. Gill, Review and comparison of active space debris capturing and removal methods, Progress in Aerospace Sciences 80 (2016) 18–32.
[146] N. R. Council and Others, Protecting the Space Shuttle from Meteoroids and Orbital Debris, National Academies Press, 1997.
[147] H. Klinkrad, Space Debris: Models and Risk Analysis, Springer Science & Business Media, 2006.
[148] S. Alfano, Review of conjunction probability methods for short-term encounters (AAS 07-148), Advances in the Astronautical Sciences 127 (1) (2007) 719.
[149] a.-P. Garc\'\i, Ricardo, J. Hernando-Ayuso, Series for collision probability in short-encounter model, Journal of Guidance, Control, and Dynamics (2016) 1908–1916.
[150] J. Hernando-Ayuso, C. Bombardelli, and J. L. Gonzalo, "Occam: optimal computation of collision avoidance maneuvers.".
[151] S. Alfano, Eliminating assumptions regarding satellite conjunction analysis, The Journal of the Astronautical Sciences 59 (4) (2012) 676–705.
[152] I. Grande-Olalla, N. Sanchez-Ortiz, J.A. Pulido, K. Merz, Collision risk assessment and avoidance manoeuvre strategies for satellites: new tool CORAM for ESA, Sixth European Space Debris Conference, vol. 1, 2013, p. 2013.
[153] R. Schneider, Convex Bodies: the Brunn-minkowski Theory, Volume 151 of Encyclopedia of Mathematics and its Applications, (2014).
[154] G. L. E. N. N. PETERSON, M. A. R. L. O. N. SORGE, W. I. L. L. I. A. M. AILOR, SPACE TRAFFIC MANAGEMENT IN THE AGE OF NEW SPACE, (2018).
[155] T.S. Kelso and others, Analysis of the iridium 33-cosmos 2251 collision, Advances in the Astronautical Sciences 135 (2) (2009) 1099–1112.
[156] T.S. Kelso, S. Alfano, Satellite orbital conjunction reports assessing threatening encounters in space (SOCRATES), Modeling, Simulation, and Verification of Space-based Systems III, vol. 6221, 2006, p. 622101.
[157] D. Vallado, P. Crawford, R. Hujsak, T.S. Kelso, Revisiting spacetrack report# 3, AIAA/AAS Astrodynamics Specialist Conference and Exhibit, 2006, p. 6753.
[158] J. Chan, Current state of conjunction monitoring for satellite operators and the steps forward, 24th International Symposium on Space Flight Dynamics, 2014.
[159] T.S. Kelso and others, Improved Conjunction Analysis via Collaborative Space Situational Awareness, (2008).
[160] D.A. Vallado, P.J. Cefola, Two-line element sets–practice and use, 63rd International Astronautical Congress, Naples, Italy, 2012.
[161] T. Flohrer, H. Krag, H. Klinkrad, ESA's process for the identification and assessment of high-risk conjunction events, Advances in Space Research 44 (3) (2009) 355–363.
[162] T.S. Kelso, How the Space Data Center Is Improving Safety of Space Operations, (2010).
[163] R.J. Rovetto, T.S. Kelso, Preliminaries of a Space Situational Awareness Ontology, (2016) 1606.01924.
[164] A.P. Cox, C.K. Nebelecky, R. Rudnicki, W.A. Tagliaferri, J.L. Crassidis, B. Smith, The space object ontology, Information Fusion (FUSION), 2016 19th International Conference on, 2016, pp. 146–153.
[165] M. Jah, et al., Space Traffic Management (STM): Balancing Safety, Innovation, and Growth, AIAA Institute Position Paper, 2017.
[166] D. Kucharski, J.C. Bennett, G. Kirchner, M.K. Jah, J.G. Webb, J. Spurbeck, High sampling rate photometry of spinning satellites for nano-perturbation detection, 2018 Advanced Maui Optical and Space Surveillance Technologies Conference (AMOS), 2018.
[167] J. Spurbeck, M.K. Jah, D. Kucharski, J.C.S. Bennett, J.G. Webb, Satellite characterization, classification, and operational assessment via the exploitation of remote photoacoustic signatures, Advanced Maui Optical and Space Surveillance Technologies Conference (AMOS), 2018.